

A Comparative Study of Multiple Approaches for Predicting the Soil–Water Retention Curve: Hyperspectral Information vs. Basic Soil Properties

Ebrahim Babaeian

Mehdi Homae*

Dep. of Soil Science
Tarbiat Modares University
Tehran, 14115-336
Iran

Harry Vereecken

Carsten Montzka

Institutes of Bio- and Geosphere
Agrosphere (IBG-3)
Forschungszentrum Jülich GmbH
52425 Jülich
Germany

Ali Akbar Norouzi

Soil Conservation and Watershed
Management Research Institute
Tehran, Iran

Martinus Th. van Genuchten

Dep. of Mechanical Engineering
COPPE/LTTC
Federal University of Rio de Janeiro
Rio de Janeiro, RJ, 21945-970
Brazil

and

Dep. of Earth Sciences
Utrecht University
Budapestlaan 4
3584 Utrecht
Netherlands

Information about the soil–water retention curve is necessary for modeling water flow and solute transport processes in soils. Soil spectroscopy in the visible, near-infrared, and shortwave infrared (Vis-NIR-SWIR) range has been widely used as a rapid, cost-effective and nondestructive technique to predict soil properties. However, less attention has been paid to predict soil hydraulic properties using soil spectral data. In this paper, spectral reflectances of soil samples from the Zanjanrood watershed, Iran, were measured in the Vis-NIR-SWIR ranges (350–2500 nm). Stepwise multiple linear regression coupled with the bootstrap method was used to construct predictive models and to estimate the soil–water retention curve. We developed point and parametric transfer functions based on the van Genuchten (VG) and Brooks-Corey (BC) soil hydraulic models. Three different types of transfer functions were developed: (i) spectral transfer functions (STFs) that relate VG/BC hydraulic parameters to spectral reflectance values, (ii) pedotransfer function (PTFs) that use basic soil data as input, and (iii) PTFs that consider spectral data and basic soil properties, further referred to as spectral pedotransfer functions (SPTFs). We also derived and evaluated point transfer functions which estimate soil–water contents at specific matric potentials. The point STFs and SPTFs were found to be accurate at low and intermediate water contents ($R^2 > 0.50$ and root mean squared error [RMSE] $< 0.018 \text{ cm}^3 \text{ cm}^{-3}$), while the point PTFs performed better close to saturation. The parametric STFs and SPTFs of both the VG and BC models performed similarly to parametric PTFs in estimating the retention curve. The best predictions of soil–water contents were obtained for all the three transfer functions when the VG and BC retention models were fitted to the retention points estimated by the point transfer functions. Overall, our findings indicate that spectral data can provide useful information to predict soil–water contents and the soil–water retention curve. However, there is a need to extend and validate the derived transfer functions to other soils and regions.

Abbreviations: BC, Brooks and Corey; EF, model efficiency; MAE, mean absolute error; PTF, pedotransfer function; RMSE, root mean squared error; SMLR, stepwise multiple linear regression; SPTF, spectral pedotransfer function; STF, spectral transfer function; VG, van Genuchten; Vis, Visible; NIR, near infrared; SWIR, shortwave infrared.

Unsaturated soil hydraulic property information is necessary for predicting and managing water flow and solute transport processes in soils. The accuracy with which these properties can be estimated has however a significant effect on the quality of predicted soil hydrological fluxes and states (Montzka et al., 2011). Pedotransfer functions are now popularly used to estimate the soil hydraulic functions from basic soil data such as the particle-size distribu-

Soil Sci. Soc. Am. J. 79:1043–1058

doi:10.2136/sssaj2014.09.0355

Received 6 Sept. 2014.

Accepted 8 Apr. 2015.

*Corresponding author(mhomae@modares.ac.ir).

© Soil Science Society of America, 5585 Guilford Rd., Madison WI 53711 USA

All rights reserved. No part of this periodical may be reproduced or transmitted in any form or by any means, electronic or mechanical, including photocopying, recording, or any information storage and retrieval system, without permission in writing from the publisher. Permission for printing and for reprinting the material contained herein has been obtained by the publisher.

tion, the bulk density, and the organic C content (Vereecken et al., 1989, 1990, 1992, 2010; Schaap et al., 1998, 2001; Jarvis et al., 2002; Rawls and Pachepsky, 2002; Pachepsky and Rawls, 2004; Pachepsky et al. 2006; Jana et al., 2007; Homaei and Farrokhan Firouzi, 2008; Weynants et al., 2009; Ghorbani Dashtaki et al., 2010). Both point and parametric PTFs have been used for this purpose. Point PTFs predict soil–water contents at specific matric potentials, while continuous PTFs predict the hydraulic functions in their entirety. Parametric PTFs have attracted more attention since they quickly provide soil hydraulic parameter estimates for use in hydrological models. By comparison, fewer studies have tried to estimate the soil hydraulic parameters by fitting retention functions to water contents obtained using point PTFs (Baumer, 1992; van den Berg et al., 1997; Tomasella and Hodnett, 1998; Tomasella et al., 2000).

In addition to basic soil data, supplementary information has been used to improve the performance of PTFs including soil structural information (Rawls and Pachepsky, 2002; Pachepsky et al., 2006; Lilly et al., 2008), the water content at selected matric potentials (Børgesen and Schaap, 2005; Børgesen et al., 2008), clay mineralogy and taxonomic information (Pachepsky and Rawls, 2004), vegetation parameters (e.g., the leaf area index or the normalized difference vegetation index) and topography attributes (e.g., elevation, slope, and aspect) (Pachepsky et al., 2001; Leij et al., 2004; Sharma et al., 2006; Jana and Mohanty, 2011).

During the past two decades, visible (Vis), near-infrared (NIR), and shortwave-infrared (SWIR) spectrometry has been widely used to estimate a range of soil properties, and also as a rapid and cheap method in digital soil mapping. Using spectral data, measurements take a few seconds, several soil properties can be estimated from a spectrum, soil analysis is cheap where high spatial density is required, sample preparation involves only drying and sieving and no (hazardous) chemicals are required. Physical soil constituents and properties that affect the bulk soil spectral reflectance the most are soil color, soil moisture, organic C, particle size and Fe- and Al- oxides (Stenberg et al., 2010). This is the fundamental principle behind using the spectral approach to estimate soil properties and its applications have been extensively reviewed (Viscarra Rossel et al., 2006c; Stenberg et al., 2010; Soriano Disla et al., 2014).

Several studies have shown the capability of laboratory scale Vis-NIR-SWIR (400–2500 nm) spectrometry to accurately predict a range of soil properties, including particle-size distribution (Gomez et al., 2008; Lagacherie et al., 2008; Janik et al., 2009; Lopez et al., 2013), soil aggregate-size distribution (Sarathjith et al., 2014a, 2014b), calcium carbonate (Lagacherie et al., 2008; Gomez et al., 2008), pH (Viscarra Rossel and Behrens, 2010), organic C content (Nocita et al., 2013; Lopez et al., 2013) and the cation-exchange capacity (Janik et al., 2009; Savvides et al., 2010). Volume-based soil properties such as bulk density are typically estimated from spectral information in an indirect manner through correlation with basic soil properties such as clay content and soil organic matter. Latter properties are often better correlated with spectral properties. Bulk density is

a key property that is required to obtain reasonable estimates of the wet part of the soil moisture retention characteristic.

In addition to estimating basic soil properties from spectral information, several studies explored the potential of using spectral information to estimate soil–water content at specific pressure head values. Janik et al. (2007), used partial least squares regression (PLSR) method to relate mid-infrared spectral data (2500–20000 nm) to soil–water contents at matric potentials of -100 and -15000 cm. They obtained coefficients of determination, R^2 , equal to 0.67 and 0.87 for these two water contents, respectively. Similarly, Minasny et al. (2008) used mid-infrared spectroscopy to predict water content at matric potential values of -10, -100, -3000, and -15000 cm. They found that water contents at the lower matric potentials (notably -15000 cm) could be estimated better ($R^2 = 0.51$, RMSE = $0.05 \text{ cm}^3 \text{ cm}^{-3}$) than those at high matric potentials (-100 cm, with $R^2 = 0.08$ and, RMSE = $0.07 \text{ cm}^3 \text{ cm}^{-3}$). Since current hyperspectral satellites operate in the Vis-NIR-SWIR range, mid-infrared spectroscopy at present cannot be used to estimate soil properties by satellite imagery. For this reason, Lagacherie et al. (2008) suggested using spectrotransfer functions that link reflectance measurements to soil properties.

Rather than only estimating specific points of the soil moisture retention characteristic, recent studies analyzed the potential of spectral soil information to estimate soil hydraulic properties using parametric PTFs. Santra et al. (2009) used principal component transformed spectral data (350–2500 nm) as well as mimicked Landstat-ETM⁺ spectral bands to estimate van Genuchten–Mualem soil hydraulic parameters (a , n , and K_s) of the wet part (> -800 cm) of the retention curve. Their results were promising for the parameter n , but they had difficulties to estimate a and K_s . One major weakness of this approach is that the soil hydraulic parameters are estimated from a limited range of measured water contents only. Also, none of the above studies (i.e., Janik et al., 2007; Minasny et al., 2008; Lagacherie et al., 2008; Santra et al., 2009) introduced clearly effective wavelengths for use in predictive models, whereas it is very important to characterize sensitive spectral regions to better understand the relation between spectral response and the physical behavior of soils. Recently, Babaeian et al. (2015) evaluated the general potential of hyper- and multi-spectral remote sensors to retrieve Mualem-van Genuchten hydraulic parameters, and tested it with laboratory- and soil-map-based HYPRES and Rosetta PTFs. Results indicate that with the upcoming hyperspectral EnMAP mission it is in principle possible to retrieve van Genuchten–Mualem soil hydraulic parameters in adequate accuracy, while the reduced spectral information of the Sentinel-2 sensor is principally not able to predict soil hydraulic parameters. The presented STF approach does not require soil texture and organic matter data, which is an advantage for areas that do not have such basic information. Based on the data set obtained by Babaeian et al. (2015), in this study we present a comparative analysis of spectral information along with simple soil data for deriving and validating different types of point and parametric

transfer functions. The innovation lies in the estimation of the VG and BC hydraulic parameters as well as soil–water contents at specific matric potentials, which are applied to predict soil–water retention characteristics.

To evaluate if visible and near-infrared spectroscopy can improve predictions of VG and BC soil hydraulic parameters, three different approaches were investigated; (i) STFs that predict hydraulic parameters from spectral reflectance data, (ii) PTFs based on soil properties such as particle-size distribution, bulk density, organic C content and geometric mean of soil particles diameter, and (iii) SPTFs that predict hydraulic parameters from the joint use of spectral reflectance data and basic soil attributes. We further evaluated point and parametric approaches to estimate VG and BC parameters using a fit of the retention models to the estimated soil–water contents and hydraulic parameters obtained with the parametric transfer functions.

MATERIALS AND METHODS

Study Area, Soil Sampling, and Soil Property Measurements

The number of disturbed and undisturbed (cores with a diameter of 6.8 cm and a height of 5 cm) soil samples ($n = 2 \times 174$) were collected from the top 30 cm soil horizon of Zanjanrood subwatershed, northwest of Iran. The soils were classified as Calcixerepts, Haploxerepts, and Xerorthents (USDA Soil Taxonomy, Soil Survey Staff, 2010b). A more detailed description of the study area is given in Babaeian et al. (2015).

Collected basic properties of the soil samples included clay (C, < 2 mm), silt (Si, 2–50 mm), sand (S, 50–2000 mm), organic carbon content (OC), and dry bulk density (ρ_b) which were measured using sedimentation (Gee and Bauder, 1986), dichromate oxidation (Walkley and Black, 1934), and paraffin coated procedures. The geometric mean of the soil particle diameter, d_g , was determined using the method of Shirazi and Boersma (1984). Gravimetric water contents were measured on the undisturbed cores at three matric potentials in the wet range (i.e., 0, -5, -10 cm) and on the disturbed samples at six matric potential in the mid (-330, -1000) and the dry (i.e., -3000, -5000, -10000, and -15000 cm) ranges of the water retention curve using sand-box apparatus (Eijkelpamp Agri-Equipment, Giesbeek, the Netherlands) and pressure plate extractor methods (Soil Moisture Equipment Corp., Santa Barbara, CA; Vereecken et al. (2010), see also Babaeian et al. (2015) for more details). The calibration and validation subsets were selected to divide the study area into a west and an east part. The data of the western part ($n = 130$) were used as calibration set. While those of the eastern part ($n = 44$) were used to provide a completely independent data set for validation of the derived transfer functions. Using independent sample t test statistics, a comparison of the mean values of the calibration and validation set confirmed no significant ($p > 0.19$) at the 0.05 significance level.

The soil–water retention functions were parameterized using the equations of van Genuchten (1980) and Brooks-Corey (Brooks and Corey, 1964), given by Eq. [1] and [2], respectively,

$$\theta(b) = \theta_r + (\theta_s - \theta_r) \left[1 + (\hat{\alpha}_{VG} |b|)^{n_{VG}} \right]^{-m} \quad [1]$$

$$\theta(b) = \theta_r + (\theta_s - \theta_r) \left[\alpha_{BC} |b| \right]^{-\lambda_{BC}} \quad [2]$$

where θ [$\text{cm}^3 \text{cm}^{-3}$] is the soil–water content at matric potential b [-cm], $\hat{\alpha}_{VG}$ [cm^{-1}] and α_{BC} [cm^{-1}] are shape parameters of the VG and BC models, respectively (approximately equivalent to the inverse of the air-entry value), n_{VG} [-] and λ_{BC} [-] are pore-size distribution parameters, m is an empirical constant that can be related to n (i.e., $m = 1 - 1/n_{VG}$), and θ_r and θ_s [$\text{cm}^3 \text{cm}^{-3}$] are the residual and saturated water contents, respectively. Using nonlinear least-squares optimization, the retention models were fitted to measured soil–water content values to obtain the hydraulic parameters, that is, α_{BC} , $\hat{\alpha}_{VG}$, n_{VG} and λ_{BC} . During the optimization process, the residual water content was found to be very close to zero, and thus it was fixed at zero for all samples (Babaeian et al., 2015).

Laboratory Hyperspectral Reflectance Measurements

The soil samples were air-dried and sieved through a 2-mm mesh sieve to obtain the fine earth fraction of soil. Spectra of the air-dried and sieved samples were recorded in the Vis-NIR-SWIR (350–2500 nm) range with 1.4 (350–100 nm) to 2 (1000–2500 nm) nm sampling intervals. The measured hydraulic parameters (i.e., water content at each matric potential, the VG and the BC retention models parameters) were then correlated with spectral reflectance data. We have not focused on the spectral reflectance measurements at different matric potentials, but measured the spectral reflectance for air-dried and sieved soil samples. These measured spectra were then used to derive STF and SPTF. Extensive research in the past showed that spectral measurement of soil on air-dried and sieved samples is a standard and routine procedure which has been widely used already at the laboratory scale (e.g., Ben-Dor and Banin, 1995; Chang et al., 2005; Brown et al., 2006; Janik et al., 2009; Santra et al., 2009; Bilgili et al., 2010; Viscarra Rossel and Behrens, 2010; Stenberg et al., 2010; Nocita et al., 2011; Lopez et al., 2013; Nocita et al., 2013). Lobell and Asner (2002) showed that soil water, when present in substantial amounts, has strong absorption bands in the NIR-SWIR range, which could interfere with the spectral features of other soil components and reduces the performance of calibration results. Although air-dried samples show a slight variation in bound water content (hygroscopic water) due to variation in texture, the inferential effect of such amount of water is negligible on spectral measurements. In such case, the interferential effect of soil moisture is negligible on spectral measurements. It was also found that sample fineness has no significant effect on the calibration results (Genot et al., 2011; Nduwamungu et al., 2009). The measurements were performed in a standard and controlled dark laboratory environment using a handheld FieldSpec3 spectroradiometer (Analytical Spectral Device, ASD, Boulder, CO).

A spectral library of 174 soil reflectance spectra, which has been described in detail in Babaeian et al. (2015), was obtained by arithmetic averaging of the iterations for each soil sample.

Transformation of the Vis-NIR-SWIR Reflectance Spectra and Preprocessing

Spectral transformations and data preprocessing were used to render the data more suitable for analysis by correcting for background effects (Viscarra Rossel, 2008), light scattering (Barnes et al., 1989), removing nonlinearities in the spectra (Viscarra Rossel, 2008) and improving calibration (Tian et al., 2013; Nocita et al., 2013; Viscarra Rossel, 2008). Various preprocessing and pretreatment algorithms can be used for this purpose, such as Savitzky-Golay and median filtering (for de-noising and smoothing of spectra), using first and second derivatives of the spectrum (to eliminate background effects; Viscarra Rossel, 2008), using standard normal variate and multiplicative scatter correction (to remove light scatter and baseline correction) (Geladi and Kowalski, 1986), and absorbance and continuum removal transformations (to reduce nonlinearities in the spectra; Lagacherie et al., 2008).

Based on cross validation, we used continuum removed spectra transformation after applying Savitzky-Golay smoothing with a second-order polynomial in segments (of the observation points) involving three points (Savitzky and Golay, 1964). More details about continuum removal methods and the Savitzky-Golay algorithm are given in the literature (Stenberg et al., 2010; Noomen et al., 2006; Lagacherie et al., 2008; Babaeian et al., 2015).

Before performing the spectral analyses, we excluded spectral data obtained in the range between 350 and 399 nm and 2451 and 2500 nm because of excessive noise (Viscarra Rossel et al., 2006c). Since spectroradiometer data are very repetitive and heavily over-sampled with a high degree of correlation between neighboring bands, data redundancy was reduced using data reduction and down-sampling. We did this by averaging every five contiguous 1-nm wavelengths resulting in 410 data points from 400 to 2450 nm for calibration (Lopez et al., 2013).

Model Development and Hydraulic Property Estimation

Hyperspectral data with high spectral resolution (1 nm) and broader wavelengths (350–2500 nm) have been used frequently for estimating soil properties (Ben-Dor and Banin, 1995; Chang et al., 2001; Islam et al., 2003; Viscarra Rossel et al., 2006a, 2006c). These spectral data always show considerable collinearity and heteroscedasticity, which should be avoided when developing PTFs based on regression equations. Characterizing relevant wavebands is hence important for developing reliable prediction models and spectral indices. For this reason, we employed correlation analysis and stepwise multiple linear regression statistics (SMLR), which allows the selection of bands that have better correlations with each attribute.

Three different approaches were used to develop pedotransfer functions: STFs, PTFs, and SPTFs (Fig. 1). These approaches are briefly summarized below.

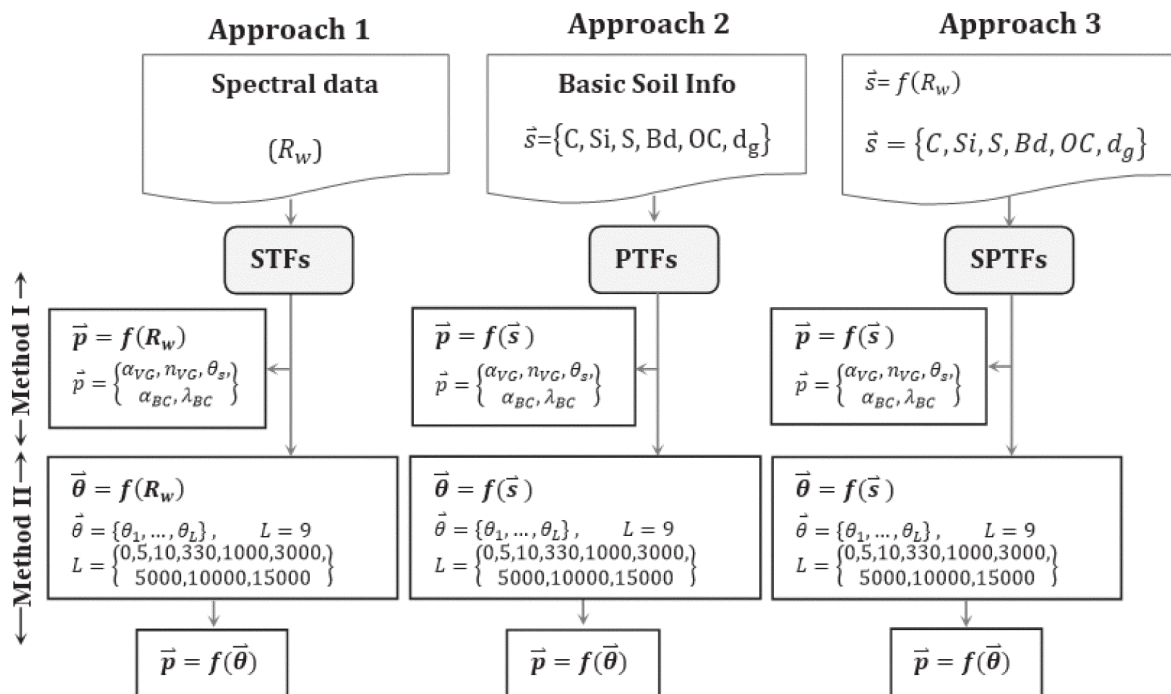


Fig. 1. Graphical representation of three approaches used to estimate hydraulic parameters from spectral data and/or basic soil information. C, Si, S, ρ_b , OC, d_g represent clay, silt, sand, bulk density, organic carbon, and geometric mean of soil particles diameter, respectively; R_w is spectral reflectance at wavelength w ; α_{VG} and n_{VG} are VG shape parameters; α_{BC} and λ_{BC} are BC shape parameters; θ_s is saturated soil-water content; θ is soil-water content; and subscript L represents a particular matric potential.

Approach 1: Spectral Transfer Functions

In the first approach, spectral reflectance values, referred to as Scenario I in Babaeian et al. (2015), were used as unique predictor variables to derive both point and parametric STFs. Point STFs estimate the vector $\bar{\theta} = \{\theta_1, \dots, \theta_L\}$ where θ refers to the soil–water content and the subscripts to matric potential levels between 1 and L . We estimated water contents at the nine available matric potentials ($L = 9$): 0, -5, -10, -330, -1000, -3000, -5000, -10000, and -15000 cm. Parametric spectral transfer functions developed in this paper estimate the unknown parameter vector $\bar{p} = \{\hat{\alpha}_{VG}, n_{VG}, \alpha_{BC}, \lambda_{BC}, \theta_s\}$ (later referred as Method I) where $\hat{\alpha}_{VG}$ and n_{VG} are VG shape parameters, α_{BC} and λ_{BC} are BC shape parameters, and θ_s is the saturated soil–water content. The STFs relate the two parameter vectors \bar{p} and $\bar{\theta}$ to spectral reflectance values using regression analysis: $\bar{p} = f(R_w)$ and $\bar{\theta} = f(R_w)$, where R_w is the spectral reflectance at wavelength w and f refers to the regression equation.

We also fitted the VG and BC retention functions to estimated soil–water contents obtained from the point STFs (i.e., $\bar{p} = f(\bar{\theta})$) to construct new sets of the VG and BC parameters (later referred as Method II; see Fig. 1) and predict soil–water retention.

Approach 2: Pedotransfer Functions

In the second approach, \bar{p} and $\bar{\theta}$ vectors are directly related to basic soil properties, i.e., $\bar{p} = f(\bar{s})$ and $\bar{\theta} = f(\bar{s})$, where $\bar{s} = \{C, Si, S, \rho_b, OC, d_g\}$ (Fig. 1), to derive parametric (Method I) and point PTFs. Like in the first approach, both retention models VG and BC were then fitted to the point PTFs (Method II). Such new set of hydraulic parameters were used to predict soil–water retention.

Approach 3: Spectral Pedotransfer Functions

The third approach is, in fact, a combination of the two previous approaches in that first, relationships between the basic soil properties (\bar{s}) and the spectral reflectance data are derived, (i.e., $\bar{s} = f(R_w)$). Then the outputs are used as input data into derived point and parametric PTFs (i.e., Approach 2) to obtain \bar{p} and $\bar{\theta}$. The VG and BC models were then fitted to the point SPTFs (i.e., Method II). Using two different sets of hydraulic parameters for each parametric transfer function (i.e., Methods I and II), water contents at specific matric potentials were generated (see Fig. 1) and were compared with measured retention points.

General Statistical Analysis for Spectral Transfer Functions, Pedotransfer Functions, and Spectral Pedotransfer Functions

Before model development, descriptive statistics of the basic soil properties and soil hydraulic parameters were calculated and tested for normality (at the 5% level of significance, $p < 0.05$) using the Kolmogorov–Smirnov one sample test statistics (Babaeian et al., 2015). Transformations were performed for those variables that did not follow a normal distribution. Pearson's correlation analyses were performed on the calibration subset to explore the

correlation between basic soil variables and hydraulic properties (i.e., water content at each matric potential or the VG and the BC retention models parameters) with the spectral reflectance data. Variables showing a strong correlation (at significance levels of 1 and 5%) with hydraulic parameters were included in SMLR as three separate sets of predictors for deriving three different sets of transfer functions (see Fig. 1). Details on the SMLR and the estimation process used are given in Babaeian et al. (2015). To avoid multicollinearity in each derived function, the 'Variance Inflation Factor', VIF, was used (Hocking, 2003; Ho, 2006). We additionally used the 'Durbin-Watson statistic' to check autocorrelation among the residuals of the regression equations (Ho, 2006; Babaeian et al., 2015).

Multiple linear regressions coupled with the bootstrap method (Efron and Tibshirani, 1993) are often used to provide robust estimates. Briefly, bootstrapping is a non-parametric technique for deriving robust estimates of regression coefficients. Bootstrapping is most useful as an alternative to parametric estimates when the assumptions of those methods are in doubt (as in the case of regression models with heteroscedastic residuals fit to small samples).

The bootstrap method creates random subsets (realizations) from a calibration set of size N to obtain B bootstrap data sets, each with size N , through repeated sampling with replacement. The bootstrap dialog box in PASW statistics was employed to specify the bootstrap analyses and to create the bootstrap samples. The simple resampling method with replacement from the original dataset, with a number of 1000 bootstrap samples, were specified at a 95% percentile confidence interval. Linear regression coupled with bootstrap provides descriptive statistics and coefficients tables that support mean, standard deviation and bootstrap estimates and significance tests for the regression coefficients.

Using the three approaches, soil–water contents at specific matric potentials, as well as the VG and BC hydraulic parameters, were estimated for both the calibration and validation data sets. To adjust the coefficients of the transfer function, the coefficients of each empirical equation (i.e., the STFs, SPTFs, and PTFs) obtained by SMLR during the first step were considered as a priori sets. The empirical coefficients of each regression equation obtained from the first step were then adjusted by minimizing the sum of squared errors between the estimates from the first step and the observed hydraulic parameters (Babaeian et al., 2015; see also Weynants et al. (2009), for more details).

Accuracy and Reliability Criteria

Accuracy may be defined as the difference between measured and predicted values of the soil hydraulic properties used in the calibration step (Guber et al., 2009; Vereecken et al., 2010). Since derived transfer functions are a set of empirical equations, a test of their accuracy should be performed using a separate dataset that is independent of the calibration set. We further define reliability as evaluating the performance of the predictions using measured values that are different from those used in model development (Vereecken et al., 2010). Reliability was tested using a validation

Table 1. Criteria for evaluating the accuracy of the transfer functions.

Statistic	Formula†	Optimal value
Mean absolute error	$MAE=(1/N-p)\sum_{i=1}^N \hat{y}_i-y_i $	0
Mean bias error	$MBE=(1/N-p)\sum_{i=1}^N\hat{y}_i-y_i$	0
Root mean squared error	$RMSE=\sqrt{(1/N-p)\sum_{i=1}^N(\hat{y}_i-y_i)^2}$	0
Coefficient of determination	$R^2=\left[\frac{\sum_{i=1}^N(\hat{y}_i-\bar{\hat{y}})(y_i-\bar{y})}{\sqrt{\sum_{i=1}^N(\hat{y}_i-\bar{\hat{y}})^2\sum_{i=1}^N(y_i-\bar{y})^2}}\right]^2$	1
Model efficiency	$EF=1-\left[\frac{\sum_{i=1}^N(\hat{y}_i-y_i)^2}{\sum_{i=1}^N(y_i-\bar{y})^2}\right]$	1

† y_i and \hat{y}_i , i th observed and predicted values; \bar{y} and $\bar{\hat{y}}$, mean of the observed and predicted values; p , number of predictors in derived functions; N , number of data pairs consisting of y_i and \hat{y}_i .

set. The goodness of fit of the point and parametric STFs, SPTFs, and PTFs was evaluated using the root mean squared error (RMSE), the mean absolute error (MAE), the mean bias error (MBE), the coefficient of determination (R^2), and the model efficiency (EF) as defined in Table 1.

RESULTS AND DISCUSSION

Soil Properties and Soil Spectra

Loam and clay loam were the predominant textural classes covering about 30 and 50% of the soils in the study area, respectively (Babaecian et al., 2015). Table 2 summarizes the

Table 2. Descriptive statistics (minimum, maximum, mean, and standard deviation) of basic soil properties, water retention parameters [$\theta(h)$], Van Genuchten (VG) and Brook-Corey (BC) hydraulic parameters for the calibration and validation sets.

Soil properties†	Calibration subset ($n = 130$)				Validation subset ($n = 44$)			
	Min.	Max.	Mean	SD	Min.	Max.	Mean	SD
USDA clay, %	15	45	28	6.6	16	40	28.5	6.6
USDA sand, %	13	63	39.4	10.3	19	62	35.9	9.1
USDA silt, %	21	52	32.6	5.4	22	43	35.5	5.0
Organic carbon, %	0.06	1.56	0.636	0.25	0.23	1.95	0.656	0.34
ρ_b , g cm ⁻³	0.95	1.26	1.11	0.06	0.97	1.22	1.096	0.06
$d_g^* [= d_g^{0.5}]$, mm ^{0.5}	0.098	0.400	0.219	0.064	0.119	0.387	0.203	0.056
θ_s , cm ³ cm ⁻³	0.407	0.608	0.507	0.048	0.375	0.572	0.492	0.047
$\theta(-5 \text{ cm})$, cm ³ cm ⁻³	0.324	0.583	0.469	0.051	0.314	0.546	0.459	0.054
$\theta(-10 \text{ cm})$, cm ³ cm ⁻³	0.299	0.552	0.439	0.048	0.284	0.509	0.432	0.052
$\theta(-330 \text{ cm})$, cm ³ cm ⁻³	0.186	0.340	0.251	0.026	0.216	0.306	0.252	0.013
$\theta(-1000 \text{ cm})$, cm ³ cm ⁻³	0.141	0.272	0.206	0.024	0.166	0.260	0.208	0.012
$\theta(-3000 \text{ cm})$, cm ³ cm ⁻³	0.119	0.261	0.167	0.022	0.130	0.208	0.165	0.009
$\theta(-5000 \text{ cm})$, cm ³ cm ⁻³	0.111	0.240	0.156	0.021	0.117	0.184	0.152	0.010
$\theta(-10000 \text{ cm})$, cm ³ cm ⁻³	0.095	0.226	0.145	0.021	0.098	0.182	0.140	0.008
$\theta(-15000 \text{ cm})$, cm ³ cm ⁻³	0.094	0.218	0.137	0.020	0.092	0.174	0.133	0.009
$\alpha_{VG} [= \ln(\alpha_{ve})]$, cm ⁻¹	-3.08	-0.92	-1.85	0.454	-2.70	-0.47	-1.76	0.493
n_{VG} , [-]	1.09	1.27	1.17	0.034	1.11	1.24	1.17	0.034
α_{BC} , cm ⁻¹	0.035	0.742	0.225	0.127	0.038	0.620	0.273	0.140
$\lambda_{BC} [= \ln(\lambda)]$, [-]	-2.49	-1.26	-1.84	0.218	-2.37	-1.45	-1.84	0.194

† ρ_b , bulk density; d_g^* , geometric mean diameter of soil particles; θ_s , saturated water content [cm³ cm⁻³]; θ , water retention at specific matric potentials [cm³ cm⁻³]; α_{VG} and n_{VG} , shape parameters of VG model; α_{BC} and λ_{BC} , shape parameters of BC model.

mean value, ranges, and standard deviations of the basic soil attributes and hydraulic parameters of both the calibration and validation subsets.

Figure 2 depicts the mean and standard deviation of the raw and the continuum removed spectra of the soil samples. Corresponding with the results from Babaecian et al. (2015), spectral reflectance values were relatively low below 700 nm (the visible region) and high for the NIR and SWIR spectral range, with maximum reflectance values being about 0.38, which represents the relatively small reflectance from the soils (the maximum reflectance value of a white reference panel is equal to 1). The soil spectral reflectance generally increases in the presence of calcium carbonate, while organic matter and soil moisture tend to reduce the reflectance.

As is clearly shown in Fig. 2, both the raw and continuum removed spectra exhibit four diagnostic absorption features around 1414, 1915, 2212, and 2340 nm (Babaecian et al., 2015). The absorption peaks near 1414 and 1915 nm are strongly associated with the bending and stretching of the hydroxyl (OH) features of hygroscopic or free water, while those near 2212 nm are due to clay mineral lattice OH features (Clark, 1999; Viscarra Rossel et al., 2006c; Viscarra Rossel and Behrens, 2010). Absorption in the Vis range (for example near 480 and 650 nm) corresponds to iron oxides, which control soil color such as red hematite and yellow goethite (Stenberg et al., 2010). The absorption peak near 2341 nm wavelength may be attributed to CO₃ groups in carbonate minerals (Gaffey, 1986; Gomez et al., 2008). It has been reported that soil CaCO₃ content has a significant effect on accuracy of point and parametric PTFs in estimating water retention (Khodaverdiloo et al., 2011). These absorption features are consistent with those found in other studies (e.g., Ben-Dor and Banin, 1995; Ben-Dor et al., 1999; Gomez et al., 2008; Santra et al., 2009; Babaecian et al., 2015).

Correlation Analysis of Variables used in Transfer Functions

We used Pearson's correlation coefficient, R , to explore correlations between basic and soil hydraulic properties with the spectral reflectance values at various wavelengths across the measured spectrum to identify the most significant variables for inclusion in the point and parametric STFs, SPTFs, and PTFs. Figure 3a shows correlation values between the soil-water contents and spectral reflectance values across the Vis, NIR, and SWIR range. Soil water retained at matric potentials of -330, -1000, -3000, -10000, and -15000 cm show maximum and significant ($p < 0.01$) correlations with the spectral reflectance values

at 587-, 1417-, 1957-, and 2307-nm wavelengths. The largest correlation coefficients were observed for water contents at matric potentials of -15000 ($R = 0.673$) and -10000 cm ($R = 0.692$), followed by -5000 ($R = 0.671$), -3000 ($R = 0.658$), -1000 ($R = 0.499$), and -330 cm ($R = 0.459$) matric potentials. For values larger than -330 cm, water contents show poor correlations ($R < 0.196$) with spectral data in the 400- to 2450-nm range (Fig. 3a). Soil-water contents generally showed a similar and close trend across all wavelengths, possibly due to positive and strong correlations among the water contents across a wide range of matric potentials. The water contents at matric potentials below -3000 cm were also significantly ($p < 0.01$) correlated with the spectral reflectance across the absorption features (i.e., negative correlations at 1414, 1915, 2212 nm and positive correlations at 2340 nm), with correlation coefficients < 0.553 . Similarly, VG and BC hydraulic parameters showed significant ($p < 0.01$) correlations with the spectral reflectances across a wide range of wavelengths, particularly in the SWIR region (Fig. 3b). The largest correlations were observed at wavelengths 2307 nm (for n_{VG} , α_{BC} and λ_{BC} with $R = -0.558$, -0.517 and 0.517 , respectively), 2317 nm (for α_{VG} with $R = 0.463$), 2347 nm (for λ_{BC} with $R = 0.326$), 2217 nm (for n_{VG} and α_{BC} with $R = 0.321$ and 0.277 , respectively), 2222 nm (for α_{VG} with $R = -0.289$), 1972 nm (for α_{VG} with $R = -0.309$), 1957 nm (for n_{VG} with $R = 0.367$) and 1417 nm (for α_{VG} , n_{VG} , and α_{BC} with $R = -0.274$, 0.290 , and 0.241 , respectively). According to the literature, peaks near 1417 nm and 1957–1972 nm indicate the influence of water bound in the inter layer lattices of clay minerals (Bishop et al., 1994; Ben-Dor and Banin, 1995). The absorption near 2217–2222 nm is due to the absorption of Al-OH, and the small absorption near 2307–2317 nm may be due to Fe-OH as Fe is substituted in the octahedral sheet (e.g., in

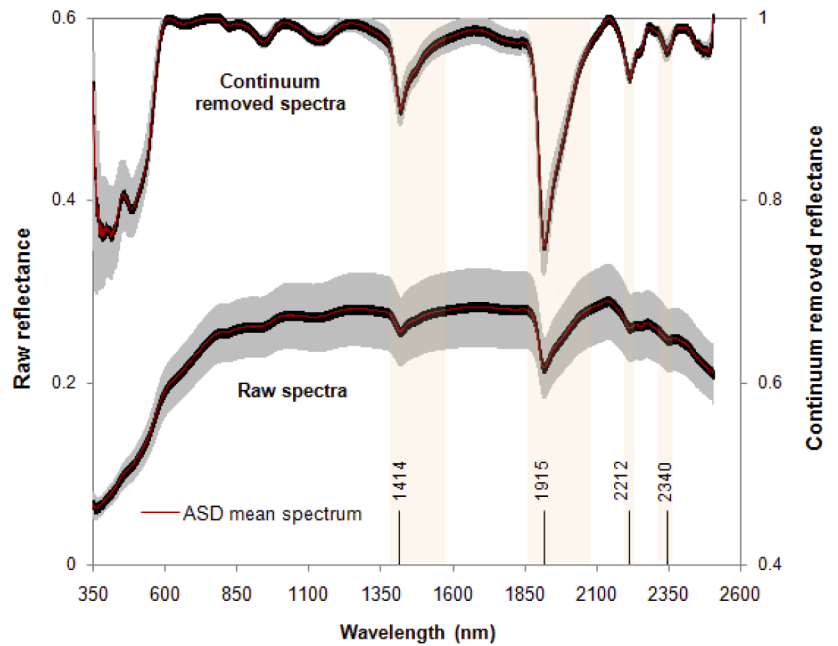


Fig. 2. Mean and standard deviation of the raw (bottom) and continuum removed (top) spectral reflectance of sampled soils for both the calibration and validation sets. Boxes depict absorption feature regions centered near 1414, 1915, 2212, and 2340 nm (Babaeian et al., 2015).

montmorillonite). The absorption near 2347 nm may represent illite or mixtures of smectite and illite (Clark et al., 1990; Post and Noble, 1993; Stenberg, 2010). In general, the weakest correlations between reflectance values and basic/hydraulic parameters were obtained at wavelengths between 800 and 1200 nm, possibly due to the lack of strong absorption features in this range.

The correlation between particle-size distribution, OC, bulk density, and the geometric mean soil particle diameter with spectral reflectance values are also shown in Fig. 3c and 3d. As reported by Babaeian et al. (2015), clay content, sand content, and silt content were significantly ($p < 0.01$) correlated with spectral reflectance values at wavelengths corresponding approximately to those of the water content values, VG and BC hydraulic parameters. Comparing Fig. 3a and 3c clearly show

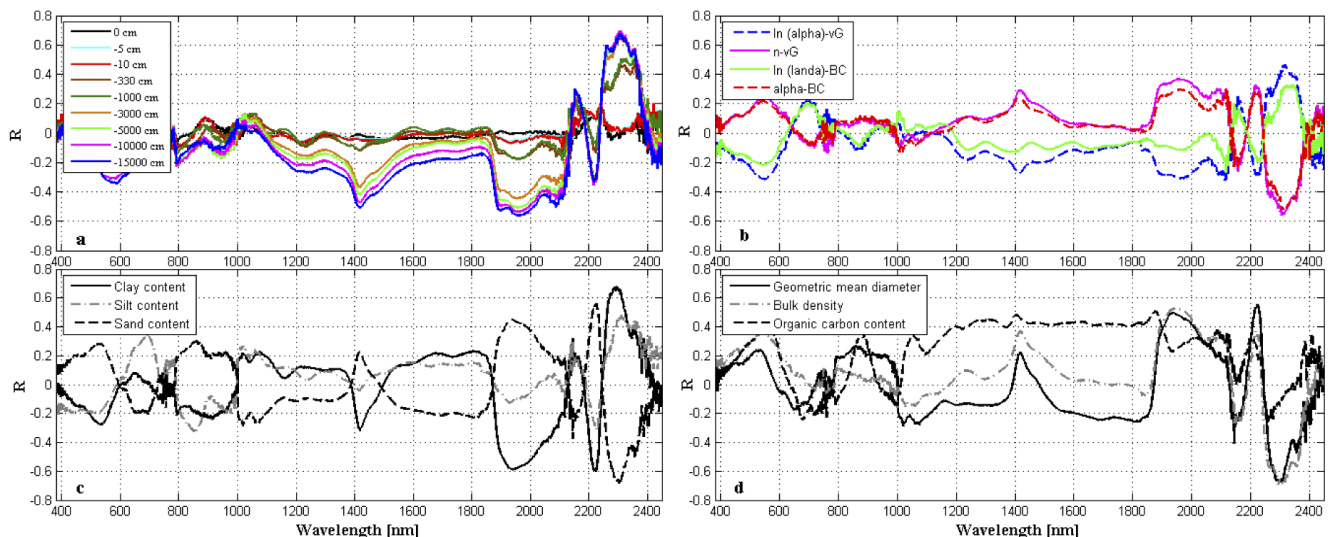


Fig. 3. Pearson's correlation coefficients between spectral reflectance values and (a) soil-water content values; (b) VG and BC hydraulic parameters; (c) clay, silt and sand content; and (d) organic carbon, bulk density and geometric mean of soil particles diameter over Vis-NIR-SWIR range.

Table 3. Pearson's correlation coefficients among hydraulic parameters, water retained at specific matric potentials and basic soil properties.†

	USDA clay	USDA sand	USDA silt	C/S, [-]	Organic C	ρ_b	d_g^*
	%				%	g cm ⁻³	[mm ^{0.5}]
α_{VG} , ln(cm ⁻¹)	0.263**	-0.294**	0.227**	0.277**	-0.164*	-0.263**	-0.276**
n_{VG} , [-]	-0.474**	0.491**	-0.338**	-0.493**	0.001	0.374**	0.477**
α_{BC} , cm ⁻¹	0.302**	-0.311**	0.212**	0.323**	-0.014	-0.257**	-0.295**
λ_{BC} , [-]	-0.538**	0.548**	-0.365**	-0.569**	-0.074	0.408**	0.533**
θ_s , m ³ m ⁻³	0.196	-0.110	-0.023	0.148	0.281*	-0.607**	-0.147
$\theta(-5\text{ cm})$, m ³ m ⁻³	0.209*	-0.133	0.004	0.171	0.231*	-0.601**	-0.165
$\theta(-10\text{ cm})$, m ³ m ⁻³	0.207*	-0.129	-0.003	0.177	0.187	-0.594**	-0.158
$\theta(-330\text{ cm})$, m ³ m ⁻³	0.450**	-0.488**	0.360**	0.514**	0.142	-0.283**	-0.467**
$\theta(-1000\text{ cm})$, m ³ m ⁻³	0.478**	-0.500**	0.350**	0.484**	0.272**	-0.359**	-0.498**
$\theta(-3000\text{ cm})$, m ³ m ⁻³	0.719**	-0.709**	0.445**	0.738**	0.201**	-0.550**	-0.706**
$\theta(-5000\text{ cm})$, m ³ m ⁻³	0.724**	-0.696**	0.416**	0.734**	0.173*	-0.561**	-0.696**
$\theta(-10000\text{ cm})$, m ³ m ⁻³	0.722**	-0.663**	0.356**	0.714**	0.144	-0.575**	-0.673**
$\theta(-15000\text{ cm})$, m ³ m ⁻³	0.705**	-0.662**	0.374**	0.710**	0.112	-0.595**	-0.662**

* indicate significant values at the 0.05 level.

** indicate significant values at the 0.01 level.

† C/S, clay to sand ratio [-]; α_{VG} and n_{VG} , shape parameters of VG model; α_{BC} and λ_{BC} , shape parameters of BC model; θ_s , saturated water content [cm³ cm⁻³]; θ , water retention at specific matric potentials [cm³ cm⁻³].

that soil–water contents below matric potential -330 cm were positively correlated with clay and silt content, while negatively correlated with sand content. One probable reason for the similar trend in correlation between the water content at low matric potentials and the clay content is that clay particles have a high adsorption energy, especially in the dry part of the retention curve, which causes more water to be retained. Similarly, the ρ_b and d_g^* were correlated with sand content, with maximum and significant ($p < 0.01$) correlation values of -0.692 and 0.505 at 2307 and 1877 nm wavelengths, respectively. Organic carbon content showed the largest and significant ($p < 0.01$) correlation at wavelengths of 1402 nm ($R = 0.480$) and 1877 nm ($R = 0.505$), which are close to the absorption features of 1414 and 1915 nm (Fig. 3d). It has been identified that the 1400- and 1900-nm wavelengths are effective for estimation of soil organic matter, while they are at the same time also characteristic for O-H and water molecules (Ben-Dor and Banin, 1995). The spectral ranges characteristics for different compounds are therefore difficult to identify with confidence (Ben-Dor et al., 1999; Brown et al., 2006; Clark, 1999; Stenberg, 2010). Significant correlations between basic soil properties and spectral reflectance values were also reported in studies by Bilgili et al. (2010), Somers et al. (2010), and Santra et al. (2009).

To develop PTFs, the correlation between basic soil properties (such as C, S, Si, OC, ρ_b and d_g^*) with the water contents and hydraulic parameters was calculated (Table 3). As an example, the largest and significant ($p < 0.01$) correlations were found between the water content at matric potential of -15000 cm and C, Si, S, ρ_b , and d_g^* , with correlation coefficients equal to 0.705, 0.374, -0.662, -0.595, and -0.662, respectively. The saturated water content only showed significant ($p < 0.01$ and 0.05) correlations with ρ_b ($R = -0.607$) and OC ($R = 0.281$). Significant ($p < 0.01$) correlations were also obtained between the VG and BC shape parameters and the particle-size

distribution and bulk density. Since both basic and hydraulic properties showed relatively high correlations with the spectral reflectance values over the Vis, NIR, and SWIR range, it may be possible to predict soil hydraulic properties using STFs and SPTFs from the available data.

Hydraulic Property Estimation Spectral Transfer Functions

Table 4 shows the coefficient of determination, R^2 , and root mean squared error, RMSE, of the derived point and parametric spectral transfer functions to predict the water content at nine matric potentials, as well as the VG and BC shape parameters, using spectral reflectance values at specific wavelengths. The point STFs yielded R^2 and RMSE values ranging between 0.02 and 0.64, and 0.012 and 0.054 cm³ cm⁻³, respectively. The parametric STFs produced R^2 values between 0.14 and 0.44. We included in this study the STFs of α_{VG} and n_{VG} from Babaeian et al. (2015) to provide a basis for comparison with the parametric PTFs and SPTFs. These results can be particularly helpful for soil hydraulic properties that do not have direct relationships with spectral reflectance data. As shown in Table 4, soil–water contents at low matric potentials are predicted with better accuracy compared to water contents in the mid and wet part of the retention curve. Better correlations between water contents at the lower matric potentials with the spectral data may be explained by the role of clay content. Clay particles have high adsorption energies, especially in the dry part of the retention curve, which causes more water to be retained, thus directly affecting soil spectral reflectance values.

Significant ($p < 0.01$) predictors for the soil–water contents and hydraulic parameters in the visible region (400–700 nm) were found in the ranges between 442 and 457 nm (blue), 502 and 587 nm (green), and 602 and 687 nm (red), which seems to represent the effects of type and content of iron oxides such

Table 4. Derived point and parametric spectral transfer functions (STFs) for predicting soil–water contents as well as van Genuchten and Brooks-Corey shape parameters, using spectral reflectance values as predictor variables. The functions express the best regression equations and their coefficient of determination, R^2 , and root mean squared error, RMSE, values.†

Spectral transfer function	R^2	RMSE
$\theta_{-15000} = -3.930+0.01 (0.123R_{442} - 0.588R_{602} - 1.749R_{662} + 5.237R_{2142} - 0.787R_{2227} + 0.909R_{2287} + 0.940R_{2327})$	0.63***	0.0126
$\theta_{-10000} = -5.427+0.01 (0.020R_{442}+0.172R_{532}-2.170R_{662}+5.278R_{2142}+0.795R_{2152}-0.543R_{2202} + 1.608R_{2307}+0.443R_{2327})$	0.64***	0.0124
$\theta_{-5000} = -0.247+0.01 (-0.0119R_{447}+0.2271R_{532}-1.832R_{677}+0.2941R_{2162}+0.4869R_{2202}+1.660R_{2307} + 0.5081R_{2322}+0.0812R_{2447})$	0.60***	0.0135
$\theta_{-3000} = -0.139+0.01 (0.0964R_{437}-1.7761R_{662}+0.0252R_{1732}-0.4809R_{2222}+0.9180R_{2302}+1.146R_{2327}-0.6940R_{2367}+1.083R_{2402})$	0.59***	0.0142
$\theta_{-1000} = -3.832+0.01 (-0.910R_{457}+1.492R_{502}-0.615R_{1162}+1.690R_{2287}+1.152R_{2332}+1.406)$	0.53***	0.0167
$\theta_{-330} = -0.354+0.01 (-0.8527 R_{437}+2.369 R_{507}-1.872 R_{572}-2.256 R_{2187}-1.975 R_{2257}+3.884 R_{2307}+1.444 R_{2422})$	0.52***	0.0178
$\theta_{-10} = -4.332+0.01 (3.386R_{2242}+1.521R_{2427})$	0.05**	0.0472
$\theta_{-5} = -4.710+0.01 (3.520R_{2242}+1.801R_{2427})$	0.05**	0.0496
$\theta_s = -2.888+0.01 (3.501R_{2242})$	0.02*	0.0536
$\alpha_{VG} = -44.107+0.01 (-2.174R_{552}+48.77R_{687} -0.494R_{1252} +0.530R_{1897}-2.608R_{2222}+19.654R_{2317}-21.71R_{2447})\S$	0.33***	0.372
$n_{VG} = 3.739+0.01 (-0.200R_{552}+0.116R_{1417} -0.385R_{1957} -1.885R_{2157}+0.935R_{2222}-2.820R_{2307}+1.623R_{2427})\S$	0.38***	0.0268
$\alpha_{BC} = 4.762+0.01 (-9.104R_{2237}+4.371R_{2347})$	0.14***	0.1172
$\lambda_{BC} = -8.813+0.01 (-4.170R_{502}+12.447R_{587} -51.518R_{2107} +48.890R_{2117}+23.261R_{2242}-22.319R_{2307})$	0.44***	0.1650

* $p < 0.001$

** $p < 0.01$

*** $p < 0.05$

† α_{VG} and n_{VG} , shape parameters of VG model; α_{BC} and λ_{BC} , shape parameters of BC model; θ_s , saturated water content [$\text{cm}^3 \text{cm}^{-3}$]; θ , water retention at specific matric potentials [$\text{cm}^3 \text{cm}^{-3}$]; R_w , spectral reflectance [%] in wavelength w in nm, R^2 and RMSE are coefficient of determination and root mean squared error, respectively.

§ Refers to Babaeian et al. (2015).

as hematite and goethite (Dematte and Garcia, 1999; Viscarra Rossel and Behrens, 2010). Potential predictor variables were also found in the NIR-SWIR range and more obviously between wavelengths of 2100 and 2400 nm where spectral reflectance values between 2107 and 2187 nm, 2202 and 2287 nm, 2302 and 2367 nm, and 2402 and 2447 nm were the significant ($p < 0.01$) variables to predict every soil–water content as well as the VG and BC shape parameters (Table 4). Soil spectral features are mainly a result of overtone absorption and combination of bond vibrations in molecules of three functional groups in minerals: OH, SO_4 , and CO_3 (Hunt and Salisbury, 1970; Ben-Dor and Banin, 1995). The main spectral features near 2160 and 2208 nm are due to the Al-OH bend plus O-H stretch combination vibrations in kaolinite (Viscarra Rossel and Behrens, 2010). The absorption features near 2280 nm may be due to Fe-OH in the octahedral sheet of clay minerals. Slight absorption near 2340, 2380, and 2450 nm represents the presence of some illite or mixtures of illite and smectite (Post and Noble, 1993; Viscarra Rossel and Behrens, 2010). The major absorption wavelengths near 1417, 1950, and 2222 nm correspond to the bending and stretching vibrations of the O–H bonds from adsorbed water and OH associated to phyllosilicates (Ben-Dor, 2002). The spectral feature centered near 2336 nm may be attributable to carbonate bands (Viscarra Rossel and Behrens, 2010). The spectral features between 1160 and 1250 nm may be due to C-H bonds within organic compounds (Stuart, 2004). We found no explanation to the spectral features obtained near 2107 nm.

The decrease in RMSE values from the wet range to the dry range of the water retention curve is in line with the results reported by Minasny et al. (2008) who used mid-infrared

spectroscopy to estimate volumetric water contents at two different matric potentials of -100 and -15000 cm. They found R^2 values of 0.08 and 0.51, and RMSEs equal to 0.07 and 0.05 $\text{m}^3 \text{m}^{-3}$, respectively. Compared with these values, however, our results are more accurate with RMSE values of 0.0126 $\text{cm}^3 \text{cm}^{-3}$ at matric potential of -15000 cm and 0.0472 $\text{cm}^3 \text{cm}^{-3}$ at matric potential of -100 cm. In a similar study, Tranter et al. (2008) used mid-infrared spectroscopy to predict particle-size distribution and bulk density. They next implemented the spectral based estimates within the PTFs as input variables and found improvements to water retention prediction by taking into account the effect of structure and adsorptive forces on water retention. They reported poor predictions of the water content of intact structured soils, particularly in the wet end of the retention curve (matric potentials 0 and -100 cm), while improved predictions were noted in the dry end (matric potential -15000 cm) where water contents are affected mainly by the adsorptive forces of soil particles.

The R^2 values obtained for estimating the a parameter of the BC model ($R^2 = 0.14$) were smaller than those obtained for water contents at low matric potentials (i.e., < -330 cm with $0.52 < R^2 < 0.63$) and the λ_{BC} parameter ($R^2 = 0.44$). Our results produced lower RMSE values (see Table 4) of the estimated VG parameters compared with findings by Santra et al. (2009) who obtained RMSE values larger than 0.06 and 1.5 for n_{VG} and the logarithmic form of $\hat{\alpha}_{VG}$, respectively. One possible reason for this poor accuracy may be attributed to the relatively narrow range of their measurements (i.e., matric potential range between 0 and -800 cm) compared with our study (full range, matric potential between 0 and 15000 cm) that were used to fit and estimate the shape parameters. When

Table 5. Derived point and parametric pedotransfer functions, PTFs, for predicting moisture retention characteristic as well as van Genuchten parameters using a set of basic soil properties as predictor variables. The functions express the best regression equations and their coefficient of determination, R^2 , and root mean squared error, RMSE, values.

Pedotransfer function†	R^2	RMSE
$\theta_{-15000} = 0.212 + 0.025 C/S - 0.087 \rho_b$	0.61***	0.0129
$\theta_{-10000} = 0.173 + 0.00088 C + 0.016 C/S - 0.061 \rho_b$	0.62***	0.0128
$\theta_{-5000} = 0.186 - 0.055\rho_b + 0.029 C/S + 0.01 OC$	0.65***	0.0126
$\theta_{-3000} = 0.153 + 0.026 C/S + 0.013 OC + 0.078d_g^*$	0.66***	0.0129
$\theta_{-1000} = 0.237 - 0.00115 S + 0.021 OC$	0.33***	0.0200
$\theta_{-330} = 0.196 + 0.020 \rho_b + 0.030 C/S + 0.013 OC$	0.29***	0.0217
$\theta_{-10} = 0.8211 - 0.2761 \rho_b + 0.00046 C$	0.36***	0.0356
$\theta_{-5} = 0.8690 - 0.2916 \rho_b + 0.0258 OC$	0.40***	0.0360
$\theta_s = 0.8690 - 0.2916 \rho_b + 0.0258 OC$	0.53***	0.0339
$\alpha_{VG} = -2.1894 + 0.020 C - 0.3199 OC$	0.10***	0.4321
$n_{VG} = 1.3312 - 0.000076 C - 0.00069 Si - 0.9998 \theta_{-15000}$	0.44***	0.0253
$\alpha_{BC} = 0.4733 - 0.1799 \rho_b + 0.00182 C - 0.002304 S$	0.10***	0.1204
$\lambda_{BC} = -1.2573 + 0.004333 S - 5.4783 \theta_{-15000}$	0.46***	0.1599

*** $p < 0.001$

† α_{VG} and n_{VG} : shape parameters of VG model; α_{BC} and λ_{BC} : shape parameters of BC model; θ_s : saturated water content [$\text{cm}^3 \text{cm}^{-3}$]; θ : water retention at specific matric potentials [$\text{cm}^3 \text{cm}^{-3}$]; ρ_b : bulk density [g cm^{-3}], d_g^* : geometric mean diameter of soil particles [$\text{mm}^{0.5}$], C, S, Si, and OC are clay, sand, silt and organic carbon content [%], respectively. R^2 and RMSE are coefficient of determination and root mean squared error, respectively.

measured data are not available for the full range of the water retention curve, the fitted parameters will have poor definition, making it difficult to estimate them with certainty.

Pedotransfer Functions

Table 5 shows the PTFs that predict soil–water contents at specific matric potentials, as well as the VG and BC hydraulic parameters. Laboratory determined clay, silt, and sand content, organic carbon content and bulk density attributes were used as predictors in the PTFs. To avoid the multicollinearity between predictor variables in the PTFs, the clay/sand ratio was utilized (Khodaverdiloo et al., 2011). Based on the derived point PTFs, soil–water contents at matric potentials between 0 and -15000 cm were predicted with R^2 and RMSE values ranging between 0.29 and 0.66 and 0.0126 and 0.0360 $\text{cm}^3 \text{cm}^{-3}$, respectively. The largest RMSE values were obtained in the wet range (i.e., -5 and -10 cm), with a mean value of 0.0358 $\text{cm}^3 \text{cm}^{-3}$, while R^2 and RMSE for saturated water

content were 0.53 and 0.0339, respectively. A large portion of this improvement at the higher matric potentials may be due to the effect of bulk density on soil–water retention close to saturation (Sharma et al., 2006; Schaap et al., 2001). This is also shown by the high coefficients of determination in the classical parametric PTFs or for point estimation of soil–water content at saturation. A review of existing point based PTFs by Vereecken et al. (2010) showed that the largest RMSE values are often obtained for water contents at matric potential values between -500 and -2500 cm (pF 2.7–3.4), with values between 0.015 and 0.037 $\text{cm}^3 \text{cm}^{-3}$. While relatively low RMSE values are found at matric potential values between -2.5 (pF 0.4, 0.011 $\text{cm}^3 \text{cm}^{-3}$) and -30 cm (pF 1.5, 0.010 $\text{cm}^3 \text{cm}^{-3}$). In this study we found greater errors in the wet range, which is in line with findings by Nemes et al. (2003) and Khodaverdiloo et al. (2011). The particular source of this sizable difference is unknown, but the narrow range in the bulk density and the organic carbon content as the input parameters may explain part of those errors. Another possible reason may be the heterogeneity of soils, loam, and clay loam being the dominant textures in the study area.

Table 5 shows that water contents are estimated with better R^2 values than the VG and BC hydraulic parameters. Like the STFs, the R^2 of the VG and BC parameters in the PTFs were less than 0.50. This may be attributed to the poor fit of VG and BC parameters to the water contents (mean RMSE value 0.014 $\text{cm}^3 \text{cm}^{-3}$), narrow range of hydraulic parameters in the dataset (e.g., n_{VG} parameter) and interdependency between the parameters (e.g., α_{VG} and n_{VG} ; α_{BC} and λ_{BC} , see Fig. 3b) (van den Berg et al., 1997; Khodaverdiloo et al., 2011). Further reasons may be the nonlinearity of the models as well as the discrepancy in dominant influences with respect to single retention points and the shape parameters which are controlled by a set of retention points. The moderate accuracy of the PTFs in this study may have been caused by the narrow range in the particle size distribution and bulk density as well as the organic carbon content (Bilgili et al. (2010), see Table 2), which leads to moderate correlation with soil–water retention values (see Table 3). Similar results for water retention predictions and hydraulic parameters using PTFs were also reported by Khodaverdiloo et al. (2011) and Tranter et al. (2008).

Table 6. The derived functions for estimating basic soil properties from spectral reflectance data, along with values of coefficient of determination, R^2 , and root mean squared error, RMSE.†

Regression equation	R^2	RMSE
$C = 6.931 + 0.01(0.4878R_{562} + 0.7998R_{617} - 7.607R_{687} + 0.1468R_{1827} - 7.654R_{2227} + 3.183R_{2327} + 3.767R_{2387})$	0.65***	0.0391
$S = -26.835 + 0.01(0.990R_{422} - 2.902R_{532} + 15.904R_{722} + 4.997R_{877} + 6.872R_{2052} - 2.402R_{2197} + 8.937R_{2222} + 7.735R_{2257} - 8.700R_{2327} - 3.838R_{2432})$	0.70***	0.0565
$Si = -30.379 + 0.01(24.757R_{762} - 2.120R_{892} + 3.100R_{2312} + 2.813R_{2407} + 2.284R_{2432})$	0.41***	0.0416
$OC = -21.98 + 0.01(2.230R_{497} - 83.661R_{677} + 77.272R_{707} + 63.858R_{772} - 52.082R_{797} + 11.854R_{1402} + 5.133R_{1862} + 7.452R_{2342} - 8.271R_{2447})$	0.69***	0.1395
$\rho_b = 5.990 + 0.01(4.925R_{677} - 1.418R_{1122} - 2.358R_{2247} - 6.215R_{2307})$	0.57***	0.0428
$d_g^* = 0.159 + 0.01(0.586R_{422} - 1.940R_{537} + 0.415R_{1917} + 2.281R_{2037} + 5.456R_{2227} - 3.821R_{2327} - 2.769R_{2432})$	0.65***	0.0383

*** $p < 0.001$.

† C, S, Si and OC: clay content [%], sand content [%], silt content [%] and organic carbon content [%], respectively; ρ_b : bulk density [g cm^{-3}], d_g^* : geometric mean diameter of soil particles [$\text{mm}^{0.5}$]; R_w : spectral reflectance [%] in wavelength w in nm.

Spectral Pedotransfer Functions

Table 6 summarizes the best regression equations for predicting basic soil properties using different sets of spectral reflectance values at specific wavelengths. The best predictions were observed for sand ($R^2 = 0.70$, RMSE = 5.65%), organic carbon ($R^2 = 0.69$, RMSE = 0.14%), clay ($R^2 = 0.65$, RMSE = 3.91%), and the geometric mean of soil particle diameter ($R^2 = 0.65$, RMSE = 0.038 mm). Bulk density and silt content were predicted with R^2 values of 0.57 and 0.41, and RMSE values equal to 0.043 g cm⁻³ and 4.16%, respectively. The R^2 and RMSE values in Table 6 are very much in line with literature values (e.g., Ben-Dor and Banin, 1995; Viscarra Rossel et al., 2006b; Wetterlind et al., 2008b; Islam et al., 2003; Chang et al., 2001; Chang and Laird, 2002; Brown et al., 2006; Minasny et al., 2008; Bilgili et al., 2010). As an example, Bilgili et al. (2010) used Vis-NIR spectral reflectance data and PLSR method to predict clay, sand, silt, and organic matter content and obtained R^2 values of 0.83, 0.70, 0.32, and 0.60, respectively. As expected, clay content was better predicted due to the spectral signatures of clay minerals typically dominating the NIR spectra (Stenberg et al., 2010). The sand fractions mainly consist of quartz and feldspars, which are relatively featureless and have a large reflectance in the Vis-NIR-SWIR range (Hunt and Salisbury, 1970). Sand and clay content are strongly correlated with each other and provide correlation coefficients that are very close to 1. The silt fraction can be assumed to be a mixture of sand and clay minerals and is therefore difficult to distinguish in the Vis-NIR-SWIR range (Wetterlind and Stenberg, 2010).

Significant ($p < 0.01$) spectral bands in the predictive models of clay, silt, and sand content occurred between 422 and 687 nm, 722 and 892 nm, 1827 and 2052 nm, 2197 and 2257 nm, and 2312 and 2432 nm wavelengths. However, it should be noted that the position of these absorption bands may slightly vary depending on the soil composition (Stenberg et al., 2010). The regression equation for organic carbon content contained spectral predictors from a wide range of wavelengths (see Table 6), which agrees with several studies that identified wavelengths near 1100, 1600, 1700 to 1800, 2000, and 2200 to 2400 nm for predicting soil organic carbon and nitrogen (Dalal and Henry, 1986; Ben-Dor and Banin, 1995; Martin et al., 2002; Stenberg, 2010). It has been reported that soil organic carbon have broad absorptions in the Vis, which are dominated by the darkness of humic acid and absorptions in the NIR-SWIR from the overtones and combination absorptions of O–H, C–H, and N–H (Clark et al., 1990; Clark, 1999). Since basic soil properties (i.e., C, S, Si, OC, ρ_b and d_g^*) were well predicted from spectral reflectance data, they were used as predictors in the PTFs for predicting soil–water content using SPTFs. Table 7 provides the accuracy of point and parametric SPTFs for predicting water contents as well as the VG and the BC hydraulic parameters. The point SPTFs provided R^2 and RMSE values ranging from 0.16 to 0.57 and 0.0145 to 0.0438 cm³ cm⁻³, respectively, with the best values obtained in the dry part of the retention curve. The parametric SPTFs gave R^2 values between 0.06 and 0.36. For the

Table 7. Accuracy of point and parametric spectral pedotransfer functions (SPTFs) for predicting soil–water contents as well as van Genuchten (VG) and Brooks-Corey (BC) parameters, using substitution of spectral reflectance based basic soil properties into the derived pedotransfer functions. Also shown are values of the coefficient of determination, R^2 , and root mean squared error, RMSE.†

	θ_{-15000}	θ_{-10000}	θ_{-5000}	θ_{-3000}	θ_{-1000}	θ_{-330}	θ_{-10}
R^2	0.57	0.56	0.56	0.53	0.33	0.22	0.16
RMSE	0.0145	0.0145	0.0149	0.0159	0.0201	0.0230	0.0406
	θ_{-5}	θ_s	α_{VG}	n_{VG}	α_{BC}	λ_{BC}	
R^2	0.20	0.23	0.13	0.36	0.06	0.34	
RMSE	0.0418	0.0438	0.4272	0.0276	0.1228	0.1781	

† θ , soil–water content at specific matric potentials [cm³ cm⁻³]; θ_s is saturated water content [cm³ cm⁻³]; α_{VG} and n_{VG} , shape parameters of VG model; α_{BC} and λ_{BC} , shape parameters of BC model.

shape parameters related to air-entry value (i.e., α), the RMSE values of the SPTFs were slightly greater than those obtained by STFs. The SPTFs performed well for the pore-size distribution parameters n_{VG} (with R^2 equal to 0.36) and λ_{BC} (with R^2 equal to 0.34). Nevertheless, the α_{BC} and α_{VG} parameters are generally estimated with very comparable degree of variation to the n_{VG} and λ_{BC} , with only exception for α_{VG} with the STFs (see Tables 4, 5, and 7).

Using SPTFs it is possible to improve prediction of properties with poor spectral response (e.g., θ_s , θ_{-5} , and θ_{-10} , see Table 4 and 7). Bulk density as the best proxy to estimate the saturated water content and the very wet range of the soil–water retention characteristics could be estimated well from spectral reflectance information (i.e., by SPTFs). In such case, it may be possible to improve the accuracy of spectral predictions near saturation using such a two-step approach. The SPTF approach, unlike PTFs, does not require soil texture and organic matter data directly. This can be regarded as an advantage for areas that do not have such basic information. Besides, the SPTF approach exploits soil spectroscopy as a cheap, rapid, and accurate provider of basic soil information, reducing the cost associated with PTF input data capture. Including spectral information in classical PTFs opens the pathway to use remotely sensed data in soil hydraulic properties estimation. Using satellite imagery-based SPTFs, like satellite imagery-based STFs, it may be possible to develop temporally dynamic PTFs to explicitly take into account the effect of soil management practices (e.g., tillage) and erosion on soil hydraulic parameter estimation.

Regression equations for water contents in the wet part of the retention curve (between 0 and -10 cm) showed the lowest R^2 (0.16–0.23) and highest RMSE (0.0406–0.0438 cm³ cm⁻³) values. The low predictability close to saturation may be because that input data (e.g., spectral-based estimated bulk density) partially capture the influence of soil structure on water retention.

Compared with STFs, the indirect prediction of water contents from spectral reflectance data (i.e., using SPTFs) yielded worse prediction accuracy in the dry and middle parts of the retention curve, with 9% higher RMSE and 14% lower R^2 . This may be due to the inherent uncertainties associated with the input parameters, which decrease the prediction accuracy.

Table 8. Validation of the derived spectral transfer functions (STFs), spectral pedotransfer functions (SPTFs), and pedotransfer functions (PTFs) for different soil–water content prediction approaches. Underlined values indicate the best performance for each transfer function.†

	MBE	MAE	RMSE	R ²	EF
First approach (STFs)					
Parametric‡					
VG §	-0.0025	0.0247	0.0350	0.934	0.9196
BC	-0.0050	0.0258	0.0361	0.929	0.9184
Point based fit¶					
VG	<u>0.0024</u>	<u>0.0227</u>	<u>0.0340</u>	<u>0.937</u>	<u>0.9345</u>
BC	0.0012	0.0248	0.0349	0.934	0.9309
Second approach (PTFs)					
Parametric					
VG	0.0104	0.0291	0.0416	0.914	0.9021
BC	0.0104	0.0281	0.0414	0.917	0.9028
Point based fit					
VG	<u>0.0084</u>	<u>0.0232</u>	<u>0.0364</u>	<u>0.932</u>	<u>0.9250</u>
BC	0.0081	0.0240	0.0368	0.930	0.9233
Third approach (SPTFs)					
Parametric					
VG	0.0106	0.0264	0.0360	0.934	0.9267
BC	0.0109	0.0271	0.0371	0.930	0.9221
Point based fit					
VG	0.0079	0.0253	0.0350	0.935	0.9306
BC	<u>0.0070</u>	<u>0.0251</u>	<u>0.0342</u>	<u>0.938</u>	<u>0.9335</u>

† MBE, mean bias error (cm³ cm⁻³); MAE, mean absolute error (cm³ cm⁻³); RMSE, root mean squared error (cm³ cm⁻³); R², determination coefficient (-); EF, model efficiency (-); VG, van Genuchten model; BC, Brooks-Corey model.

‡ Parametric transfer functions using Method I.

§ Point transfer functions-based fit using Method II.

¶ Refers to Babaeian et al. (2015).

Reliability of the Transfer Functions

Table 8 provides a quantitative comparison of the performance and reliability of the different approaches for predicting the water retention curve of the validation dataset. As indicated, all transfer functions provided R² and EF, greater than 0.90. The parametric STFs and SPTFs of both the VG and BC models developed from spectral data performed similarly to the parametric PTFs in predicting the soil–water retention curve, which validates the use of spectral data to estimate soil hydraulic properties. Several studies have shown the potential of predictors such as clay mineralogy and taxonomic information for accurate prediction of soil hydraulic properties (e.g., Pachepsky and Rawls, 2004) which have not yet been fully implemented within today's PTF models. Besides, soil spectroscopy has been successfully used to reflect the effects of soil minerals. Soil minerals (type, proportions and concentrations) such as iron oxides (e.g., goethite, hematite), clay minerals (e.g., kaolin, montmorillonite [smectite], illite) and carbonates (e.g., calcite, gibbsite) ultimately determine important properties of a soil such as texture, structure, cation exchange capacity (CEC), and specific surface area (Ben-Dor and Banin, 1995; Stenberg et al., 2010). The STF/SPTF approaches can take into account such attributes to provide more accurate soil hydraulic parameters in this respect. Various studies have shown that some important

soil properties, for example bulk density, could be obtained from some other basic soil attributes such as particle-size distribution and organic carbon content (Martin et al., 2009). This may be due to connection between bulk density and organic carbon (e.g., Rawls, 1983; Manrique and Jones, 1991; Heuscher et al., 2005), which substantially affect spectral information. Bulk density, as a proxy for soil structure, is a good predictor for the saturated water content as shown in many PTFs and soil studies (e.g., Vereecken et al., 1989; Schaap et al., 1998).

The good performance of spectral based transfer functions may also be due to the sensitivity of Vis-NIR-SWIR to many organic and inorganic components affecting soil hydraulic properties and providing accurate predictions of soil–water retention. A major advantage of spectral data for soil analysis is that from a single spectrum many properties may be accurately determined, thus offering the possibility for considerable cost savings and increased efficiency over conventional laboratory analysis.

As given in Table 8, the best predictions were obtained with the fit of the retention models to water contents estimated with point transfer functions (i.e., using Method II). We furthermore compared measured soil–water contents with values predicted with the three approaches using Methods I and II for the entire water retention curve. Results are displayed in Fig. 4 and 5 for the VG model and BC model, respectively. The validation of the transfer functions yielded comparable results to their respective calibration performance. All transfer functions for the VG and BC models provided reasonable accuracy in the mid and dry parts of the retention curve for both calibration (Fig. 4a, 4b, 5a, and 5b) and validation (Fig. 4c, 4d, 5c, and 5d) sets, while relatively poor predictions were obtained at high matric potentials, which are a lot more scattered around the 1:1 diagonal. Using the VG model and at the wet end (pF ≤ 1), the SPTFs (with RMSE = 0.0520 and 0.0527 for Methods I and II, respectively), the STFs (with RMSE = 0.0550 and 0.0548 for Methods I and II, respectively) and the PTFs (with RMSE = 0.0606 and 0.0583 for Methods I and II, respectively) performed similarly in terms of RMSE (see Table 9). Using the BC model and at pF ≤ 1, the highest (0.0642, Method I) and lowest (0.0518, Method II) RMSE values were produced by the PTFs and SPTFs, respectively. Similar results were obtained at the dry end (pF ~ 4.2) (Fig. 4c-d, see Table 9). The BC model was found to perform equally well in some cases, and the best performances at the dry end (pF ~ 4.2) were obtained with the PTFs and STFs, followed by the SPTFs. RMSE values for pF ≤ 1 were, on average, 3.9 times greater than for pF ~ 4.2, which raises concerns about predicting the wet range and the precise determination of soil–water content at matric potentials close to saturation (Vereecken et al., 2010).

Overall, all transfer functions slightly overestimated the water contents, particularly in the wet range (i.e., pF ≤ 1, with MBE 0.0017 for STFs, 0.0138 for SPTFs, and 0.0234 for PTFs) of the retention curve (data not shown). Using the VG model, the MBE varied between -0.0025 and 0.0106, with the largest value being for the parametric SPTF (Method I) and the smallest

one for the STFs (Method II). Evaluation of the MBE for the BC model showed similar results to the VG model (ranged from -0.0025 to 0.0106), with a large MBE equal to 0.0109 for parametric SPTFs and a slight decrease (MBE = 0.0012) for STFs (method II) (see Table 8).

CONCLUSIONS

In this paper we used three different approaches to derive point and parametric transfer functions from spectral data in the Vis-NIR-SWIR region and basic soil properties. Using stepwise multiple linear regression coupled with bootstrapping, we derived and evaluated three types of point and parametric transfer functions: (i) STFs, (ii) PTFs, and (iii) SPTFs which respectively used spectral data, basic soil properties and spectral based basic soil predictions as their inputs. We further evaluated a fit of the VG and BC retention models to the predicted water contents obtained with each approach.

Soil-water contents, the VG and BC parameters as well as basic soil properties showed significant ($p < 0.01$) correlation with spectral reflectance values, especially for the SWIR region. The point STFs and SPTFs performed similarly to the point PTFs in terms of R^2 and RMSE in estimating water contents in the mid and dry parts of the retention curve. In the wet range, PTFs were found to perform better than the other two approaches. Compared to the STFs, however, better water content estimates were obtained using the SPTFs in the wet range.

For the VG and BC shape parameters related to air entry value (i.e., α_{VG} and α_{BC}), the best estimations were obtained by the STFs, followed by SPTFs and PTFs that performed similarly to each other. However, for the parameters that reflect the pore-size distribution (i.e., n_{VG} and λ_{BC}), the PTFs performed better, followed by the STFs.

The parametric STFs and SPTFs (Method I) of both the VG and BC models developed from spectral data performed similar to parametric PTFs for the retention curve. This conclusion is important in that it indicates the feasibility of using spectral data to predict hydraulic properties. The best predictions were obtained with a fit of the retention models to soil-water contents estimated with point transfer functions (Method II).

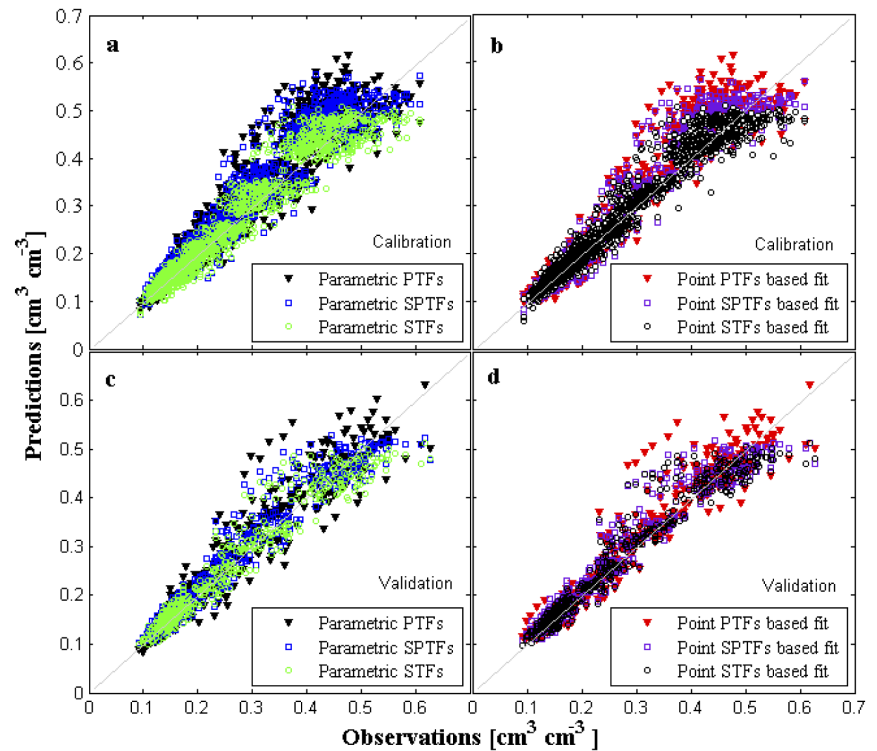


Fig. 4. Scatter plots of observed versus predicted water contents at matric potentials of 0, -5, -10, -330, -1000, -3000, -5000, -10000 and -15000 cm (all together) using parametric (left) and point (right) transfer function for the van Genuchten retention model as applied to the calibration (top) and validation (bottom) sets. The solid lines indicate 1:1 diagonals. The “parametric STFs” originated from Babaeian et al. (2015).

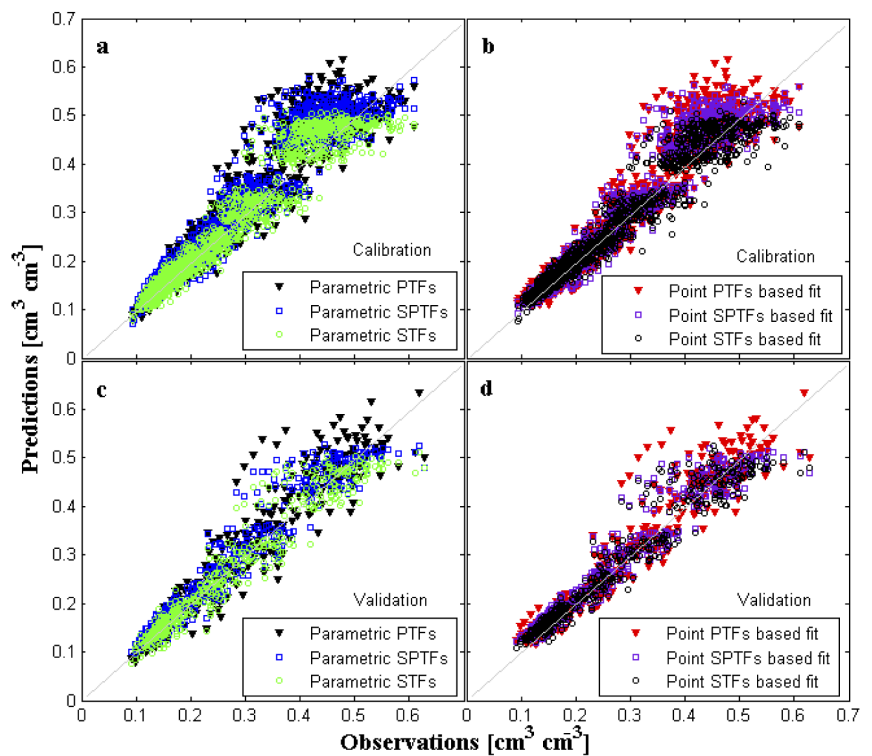


Fig. 5. Scatter plots of observed versus predicted water contents at matric potentials of 0, -5, -10, -330, -1000, -3000, -5000, -10000 and -15000 cm (all together) using parametric (left) and point (right) transfer function for the Brooks-Corey retention model as applied to the calibration (top) and validation (bottom) sets. The solid lines indicate 1:1 diagonals. The “parametric STFs” originated from Babaeian et al. (2015).

Table 9. Validation of different approaches and methods at the wet and dry ends of the soil–water retention curve in terms of RMSE.

	pF ≤ 1	pF~4.2
First approach (STFs)		
Parametric†		
VG‡	0.0550	0.0145
BC	0.0537	0.0158
Point based fits§		
VG	0.0548	0.0125
BC	0.0554	0.0140
Second approach (PTFs)		
Parametric		
VG	0.0606	0.0141
BC	0.0642	0.0125
Point based fit		
VG	0.0583	0.0114
BC	0.0593	0.0153
Third approach (SPTFs)		
Parametric		
VG	0.0520	0.0154
BC	0.0551	0.0170
Point based fit		
VG	0.0527	0.0151
BC	0.0518	0.0165

† Method I.

‡ Refers to Babaeian et al. (2015)

§ Method II

Our findings suggest that spectral information, as a promising approach, may be used to predict soil–water contents, and indirectly the water retention curve. Our results are based on a relatively local database from Iran. More variability in the basic soil properties could affect the performance of the presented relationships, and thus a definite need exists to evaluate the derived transfer functions on soils from other regions. Despite the geographic restriction of the presented STFs/SPTFs, the method we have developed can serve as a guide for future enhancements of such functions. Reflectance of a soil is a dynamic soil property that can undergo rapid changes due to change in soil composition, soil erosion, and biological processes. Using spectral data as an input of PTFs offers a way of including this temporal dynamic soil property in soil–water retention predictions. Further research could focus on evaluating spectral-based transfer functions for different soils in other regions, as well as improvement in the predictions near saturation by including the effect of structure in the predictive models. A topic of further research is the potential of STFs/SPTFs to retrieve soil hydraulic parameters at large scale and further investigation through airborne/space-borne hyperspectral remote sensing.

ACKNOWLEDGMENTS

This research was funded by Tarbiat Modares University, Iran. Ebrahim Babaeian is grateful for support from the Research Center Jülich, Agrosphere Institute (IBG-3), Germany. The authors are really grateful to the associate editor, and the two anonymous reviewers for their constructive and insightful comments, which led to a significant improvement of this paper.

REFERENCES

- Babaeian, E., M. Homaee, C. Montzka, H. Vereecken, and A.A. Norouzi. 2015. Towards retrieving soil hydraulic properties by hyperspectral remote sensing. *Vadoze Zone J.* 14: doi:10.2136/vzj2014.07.0080.
- Barnes, R.J., M.S. Dhanoa, and S.J. Lister. 1989. Standard normal variate transformation and de-trending of near-infrared diffuse reflectance spectra. *Appl. Spectrosc.* 43:772–777. doi:10.1366/0003702894202201
- Baumer, O.W. 1992. Predicting unsaturated hydraulic parameters. In: M.Th. van Genuchten et al., editors, *Indirect methods for estimating the hydraulic properties of unsaturated soils*. U.S. Salinity Lab., Riverside, CA, p. 341–355.
- Ben-Dor, E. 2002. Quantitative remote sensing of soil properties. *Adv. Agron.* 75:173–243. doi:10.1016/S0065-2113(02)75005-0
- Ben-Dor, E., J.R. Irons, and G.F. Epema. 1999. *Soil reflectance in remote sensing for the earth sciences: Manual of remote sensing*, John Wiley & Sons, New York.
- Ben-Dor, E., and A. Banin. 1995. Near infrared analysis as a rapid method to simultaneously evaluate several soil properties. *Soil Sci. Soc. Am. J.* 59:364–372. doi:10.2136/sssaj1995.03615995005900020014x
- Bilgili, A.V., H.M. van Es, F. Akbas, A. Durka, and W.D. Hively. 2010. Visible near-infrared reflectance spectroscopy for assessment of soil properties in a semi arid area of Turkey. *Arid Environ.* 74:229–238. doi:10.1016/j.jaridenv.2009.08.011
- Bishop, J.L., C.M. Pieters, and J.O. Edwards. 1994. Infrared spectroscopic analyses on the nature of water in montmorillonite. *Clay Miner.* 42:702–716. doi:10.1346/CCMN.1994.0420606
- Børgesen, C.D., B.V. Iversen, O.H. Jacobsen, and M.G. Schaap. 2008. Pedotransfer functions estimating soil hydraulic properties using different soil parameters. *Hydrol. Processes* 22:1630–1639. doi:10.1002/hyp.6731
- Børgesen, C.D., and M.G. Schaap. 2005. Point and parameter pedotransfer functions for water retention predictions for Danish soils. *Geoderma* 127:154–167.
- Brooks, R.H., and A.T. Corey. 1964. Hydraulic properties of porous media. Hydrology pap. no. 3. Colorado State University, Fort Collins, CO.
- Brown, D.J., K.D. Shepherd, M.G. Walsh, M. Dewayne Mays, and T.G. Reinsch. 2006. Global soil characterization with VNIR diffuse reflectance spectroscopy. *Geoderma* 132:273–290. doi:10.1016/j.geoderma.2005.04.025
- Chang, G.W., D.A. Laird, and G.R. Hurburgh. 2005. Influence of soil moisture on near-infrared reflectance spectroscopy measurement of soil properties. *Soil Sci.* 170:244–255. doi:10.1097/00010694-200504000-00003
- Chang, C.W., and D.A. Laird. 2002. Near-infrared reflectance spectroscopic analysis of soil C and N. *Soil Sci.* 167:110–116. doi:10.1097/00010694-200202000-00003
- Chang, C.W., D.A. Laird, M.J. Mausbach, and C.R. Hurburgh. 2001. Near-infrared reflectance spectroscopy-principal components regression analysis of soil properties. *Soil Sci. Soc. Am. J.* 65:480–490. doi:10.2136/sssaj2001.652480x
- Clark, R.N. 1999. *Spectroscopy of rocks and minerals, and principles of spectroscopy*. John Wiley & Sons, New York.
- Clark, R.N., T.V.V. King, M. Klejwa, G.A. Swayze, and N. Vergo. 1990. High spectral resolution reflectance spectroscopy of minerals. *J. Geophys. Res.* 95:12653–12680. doi:10.1029/JB095iB08p12653
- Dalal, R.C., and R.J. Henry. 1986. Simultaneous determination of moisture, organic carbon and total nitrogen by near infrared reflectance spectrophotometry. *Soil Sci. Soc. Am. J.* 50:120–123. doi:10.2136/sssaj1986.03615995005000010023x
- Dematte, J.A.M., and G.J. Garcia. 1999. Alteration of soil properties through a weathering sequence as evaluated by spectral reflectance. *Soil Sci. Soc. Am. J.* 63:327–342. doi:10.2136/sssaj1999.03615995006300020010x
- Efron, B., and R.J. Tibshirani. 1993. *An introduction to the bootstrap: Monographs on statistics and applied probability*. Chapman and Hall, CRC Press, London.
- Gaffey, S.J. 1986. Spectral reflectance of carbonate minerals in the visible and near-infrared (0.35–2.55 mm): Calcite, aragonite and dolomite. *Am. Mineral.* 71:151–162.
- Gee, G.W., and J.W. Bauder. 1986. Particle size analysis by hydrometer: a simplified method for routine textural analysis and a sensitivity tests of measured parameters. *Soil Science Soc. Am. J.* 43:1004–1007.
- Geladi, P., and B.R. Kowalski. 1986. Partial least-squares regression: A tutorial. *Anal. Chim. Acta* 185:1–17. doi:10.1016/0003-2670(86)80028-9
- Genot, V., G. Colinet, L. Bock, D. Vanvyve, Y. Reusen, and P. Dardenne. 2011.

- Near-infrared reflectance spectroscopy for estimating soil characteristics valuable in the diagnosis of soil fertility. *J. Near Infrared* 19(Spec.):117–138. doi:10.1255/jnirs.923
- Ghorbani Dashtaki, Sh., M. Homae, and H. Khodaverdiloo. 2010. Derivation and validation of pedotransfer functions for estimating soil water retention curve using a variety of soil data. *Soil Use Manage.* 26:68–74. doi:10.1111/j.1475-2743.2009.00254.x
- Gomez, C., P. Lagacherie, and G. Coulouma. 2008. Continuum removal versus PLSR method for clay and calcium carbonate content estimation from laboratory and airborne hyperspectral measurements. *Geoderma* 148:141–148. doi:10.1016/j.geoderma.2008.09.016
- Guber, A.K., Ya.A. Pachepsky, M.Th. van Genuchten, J. Simunek, D. Jacques, A. Nemes, T.J. Nicholson, and R.E. Cady. 2009. Multimodel simulation of water flow in a field soil using pedotransfer functions. *Vadose Zone J.* 8:1–10. doi:10.2136/vzj2007.0144
- Heuscher, S.A., C.C. Brandt, and P.M. Jardine. 2005. Using soil physical and chemical properties to estimate bulk density. *Soil Sci. Soc. Am. J.* 69:51–56.
- Ho, R. 2006. *Handbook of univariate and multivariate data analysis with IBM SPSS*. CRC Press, Boca Raton, FL.
- Hocking, R. 2003. *Methods and applications of linear models*. John Wiley & Sons, Hoboken, NJ.
- Homae, M., and A. Farrokhan Firouzi. 2008. Deriving point and parametric pedotransfer functions of some gypsiferous soils. *Aust. J. Soil Res.* 46:219–227. doi:10.1071/SR07161
- Hunt, G.R., and J.W. Salisbury. 1970. Visible and near-infrared spectra of minerals and rocks. I. Silicate minerals. *Mod. Geol.* 1:283–300.
- Islam, K., B. Singh, and A.B. McBratney. 2003. Simultaneous estimation of various soil properties by ultra-violet, visible and near-infrared reflectance spectroscopy. *Aust. J. Soil Res.* 41:1101–1114. doi:10.1071/SR02137
- Jana, R.B., and B. Mohanty. 2011. Enhancing PTFs with remotely sensed data for multi-scale soil water retention estimation. *J. Hydrol.* 399:201–211. doi:10.1016/j.jhydrol.2010.12.043
- Jana, R.B., B. Mohanty, and E.P. Springer. 2007. Multiscale pedotransfer functions for soil water retention. *Vadose Zone J.* 6:868–878. doi:10.2136/vzj2007.0055
- Janik, L.J., S.T. Forrester, and A. Rawson. 2009. The prediction of soil chemical and physical properties from mid-infrared spectroscopy and combined partial least-squares regression and neural networks (PLS-NN) analysis. *Chemom. Intell. Lab. Syst.* 97:179–188. doi:10.1016/j.chemolab.2009.04.005
- Janik, L.J., R.H. Merry, S.T. Forrester, D.M. Lanyon, and A. Rawson. 2007. Rapid prediction of soil water retention using mid infrared spectroscopy. *Soil Sci. Soc. Am. J.* 71:507–514. doi:10.2136/sssaj2005.0391
- Jarvis, N.J., L. Zavatiaro, K. Rajkai, W.D. Reynolds, P.A. Olsen, M. McGechan, M. Mecke, B. Mohanty, P.B. Leeds-Harrison, and D. Jacques. 2002. Indirect estimation of near-saturated hydraulic conductivity from readily available soil information. *Geoderma* 108:1–17. doi:10.1016/S0016-7061(01)00154-9
- Khodaverdiloo, H., M. Homae, M.Th. van Genuchten, and S. Ghorbani Dashtaki. 2011. Deriving and validating pedotransfer functions for some calcareous soils. *J. Hydrol.* 399:93–99. doi:10.1016/j.jhydrol.2010.12.040
- Lagacherie, P., F. Baret, J.B. Feret, J. Madeira Netto, and J.M. Robbez-Masson. 2008. Estimation of soil clay and calcium carbonate using laboratory, field, and airborne hyperspectral measurements. *Remote Sens. Environ.* 112(3):825–835. doi:10.1016/j.rse.2007.06.014
- Leij, F.J., N. Romano, M. Palladino, M.G. Schaap, and A. Coppola. 2004. Topographical attributes to predict soil hydraulic properties along a hillslope transect. *Water Resour. Res.* 40:W02407. doi:10.1029/2002WR001641
- Lilly, A., A. Nemes, J.W. Rawls, and Ya.A. Pachepsky. 2008. Probabilistic approach to the identification of input variables to estimate hydraulic conductivity. *Soil Sci. Soc. Am. J.* 72:16–24. doi:10.2136/sssaj2006.0391
- Lobell, D.B., and G.P. Asner. 2002. Moisture effects on soil reflectance. *Soil Sci. Soc. Am. J.* 66:722–727. doi:10.2136/sssaj2002.7220
- Lopez, L. R., Behrens, T., Schmidt, K., Stevens, A., Alexandre, J., Dematte, M. and Scholten, T. 2013. The spectrum-based learner: A new local approach for modeling soil vis–NIR spectra of complex datasets. *Geoderma* 195:268–279. doi:10.1016/j.geoderma.2012.12.014
- Manrique, L.A., and C.A. Jones. 1991. Bulk density of soils in relation to soil physical and chemical properties. *Soil Sci. Soc. Am. J.* 55:476–481. doi:10.2136/sssaj1991.03615995005500020030x
- Martin, M.P., D. Lo Seen, L. Boulonne, C. Jolivet, K.M. Nair, G. Bourgeon, and D. Arrouays. 2009. Optimizing Pedotransfer functions for estimating soil bulk density using boosted regression trees. *Soil Sci. Soc. Am. J.* 73:485–493. doi:10.2136/sssaj2007.0241
- Martin, P.D., D.F. Malley, G. Manning, and L. Fuller. 2002. Determination of soil organic carbon and nitrogen at the field level using near-infrared spectroscopy. *Can. J. Soil Sci.* 82:413–422. doi:10.4141/S01-054
- Minasny, B., A.B. Mc Bratney, G. Tranter, and B.W. Murphy. 2008. Using soil knowledge for the evaluation of mid-infrared diffuse reflectance spectroscopy for predicting soil physical and mechanical properties. *Eur. J. Soil Sci.* 59:960–997. doi:10.1111/j.1365-2389.2008.01058.x
- Montzka, C., H. Moradkhani, L. Weihermuller, H.J.H. Franssen, M. Canty, and H. Vereecken. 2011. Hydraulic parameters estimation by remotely-sensed top soil moisture observations with the particle filter. *J. Hydrol.* 399:410–421. doi:10.1016/j.jhydrol.2011.01.020
- Nduwamungu, C., N. Ziadi, G.F. Tremblay, and L.E. Parent. 2009. Near-Infrared Reflectance Spectroscopy Prediction of Soil Properties: Effects of Sample Cups and Preparation. *Soil Sci. Soc. Am. J.* 73:1896–1903. doi:10.2136/sssaj2008.0213
- Nemes, A., M.G. Schaap, and J.H.M. Wosten. 2003. Functional evaluation of pedotransfer functions derived from different scales of data collection. *Soil Sci. Soc. Am. J.* 67:1093–1102. doi:10.2136/sssaj2003.1093
- Nocita, M., A. Stevens, C. Noon, and B. van Wesemael. 2013. Prediction of soil organic carbon for different levels of soil moisture using Vis-NIR spectroscopy. *Geoderma* 199:37–42. doi:10.1016/j.geoderma.2012.07.020
- Nocita, M., L. Kooistra, M. Bachmann, A. Müller, M. Powell, and S. Weel. 2011. Predictions of soil surface and topsoil organic carbon content through the use of laboratory and field spectroscopy in the Albany Thicket Biome of Eastern Cape Province of South Africa. *Geoderma* 167–168:295–302.
- Noomen, M.F., A.K. Skidmore, F.D. van der Meer, and H.H.T. Prins. 2006. Continuum removed band depth analysis for detecting the effects of natural gas, methane and ethane on maize reflectance. *Remote Sens. Environ.* 105:262–270. doi:10.1016/j.rse.2006.07.009
- Pachepsky, Ya.A., and W.J. Rawls. 2004. Development of pedotransfer functions in soil hydrology. *Dev. Soil Sci.* 30. Elsevier, Amsterdam.
- Pachepsky, Ya.A., and W.J. Rawls. 2004. Development of pedotransfer functions in soil hydrology. *Developments in Soil Science*, 30, Elsevier, Amsterdam.
- Pachepsky, Y., W.J. Rawls, and D. Gimenez. 2001. Comparison of soil water retention at field and laboratory scales. *Soil Sci. Soc. Am. J.* 65:460–462. doi:10.2136/sssaj2001.652460x
- Pachepsky, Ya.A., W.J. Rawls, and H.S. Lin. 2006. Hydropedology and pedotransfer functions. *Geoderma* 131:308–316. doi:10.1016/j.geoderma.2005.03.012
- Post, J.L., and P.N. Noble. 1993. The near-infrared combination band frequencies of dioctahedral smectites, micas, and illites. *Clay Miner.* 41:639–644. doi:10.1346/CCMN.1993.0410601
- Rawls, W.J., and Ya.A. Pachepsky. 2002. Using field topographic descriptors to estimate soil water retention. *Soil Sci.* 167:423–435. doi:10.1097/00010694-200207000-00001
- Rawls, W.J. 1983. Estimating soil bulk density from particle size analysis and organic matter content. *Soil Sci.* 135:123–125. doi:10.1097/00010694-198302000-00007
- Santra, P., R.N. Sahoo, B.S. Das, R.N. Samal, A.K. Pattanaik, and V.K. Gupta. 2009. Estimation of soil hydraulic properties using proximal spectral reflectance in visible, near-infrared, and shortwave-infrared (VIS–NIR–SWIR) region. *Geoderma* 152:338–349. doi:10.1016/j.geoderma.2009.07.001
- Sarathjith, M.C., B.S. Das, H.B. Vasava, B. Mohanty, A.S. Sahadevan, P.W. Suhas, and K.L. Sahrawat. 2014a. Diffuse reflectance spectroscopic approach for the characterization of soil aggregate size distribution. *Soil Sci. Soc. Am. J.* 78:369–376. doi:10.2136/sssaj2013.08.0377
- Sarathjith, M.C., B.S. Das, S.P. Wani, and K.L. Sahrawat. 2014b. Dependency measures for assessing the co-variation of spectrally active and spectrally inactive soil properties in diffuse reflectance spectroscopy. *Soil Sci. Soc. Am. J.* 78:1522–1530. doi:10.2136/sssaj2014.04.0173
- Savitzky, A., and M.J.E. Golay. 1964. Smoothing and differentiation of data by simplified least squares procedures. *Anal. Chem.* 36:1627–1638. doi:10.1021/ac60214a047
- Savvides, A., R. Corstanje, S.J. Baxter, B.J. Rawlins, and R.M. Lark. 2010. The relationship between diffuse spectral reflectance of the soil and its cation exchange capacity is scale dependent. *Geoderma* 154:353–358. doi:10.1016/j.geoderma.2009.11.007
- Schaap, M.G., F.J. Leij, and M.Th. van Genuchten. 2001. ROSETTA: A

- computer program for estimating soil hydraulic parameters with hierarchical pedotransfer functions. *J. Hydrol.* 251:163–176. doi:10.1016/S0022-1694(01)00466-8
- Schaap, M.G., F.J. Leij, and M.Th. van Genuchten. 1998. Neural network analysis for hierarchical prediction of soil hydraulic properties. *Soil Sci. Soc. Am. J.* 62:847–855.
- Sharma, S.K., B.P. Mohanty, and J.T. Zhu. 2006. Including topography and vegetation attributes for developing pedotransfer functions. *Soil Sci. Soc. Am. J.* 70:1430–1440. doi:10.2136/sssaj2005.0087
- Shirazi, M.A., and L. Boersma. 1984. A unifying quantitative analysis of soil texture. *Soil Sci. Soc. Am. J.* 48:142–147. doi:10.2136/sssaj1984.03615995004800010026x
- Soil Survey Staff. 2010b. Keys to soil taxonomy. 11th ed. USDA–NRCS Agri. Handb., USDA–NRCS, Washington, DC.
- Somers, B., V. Gysels, W.W. Verstraeten, S. Delalieux, and P. Coppin. 2010. Modelling moisture-induced soil reflectance changes in cultivated sandy soils: A case study in citrus orchards. *Eur. J. Soil Sci.* 61:1091–1105. doi:10.1111/j.1365-2389.2010.01305.x
- Soriano-Disla, J.M., L.J. Janik, R.A. Viscarra Rossel, L.M. MacDonald, and M.J. McLaughlin. 2014. The performance of visible, near- and mid-infrared reflectance spectroscopy for prediction of soil physical, chemical, and biological properties. *Appl. Spectrosc. Rev.* 49:2, 139–186. doi:10.1080/05704928.2013.811081
- Stenberg, B., R.A. Viscarra Rossel, A.M. Mouazen, and J. Wetterlind. 2010. Visible and near infrared spectroscopy in soil science. *Adv. Agron.* 107:163–215. doi:10.1016/S0065-2113(10)07005-7
- Stenberg, B. 2010. Effects of soil sample pretreatments and standardized rewetting as interacted with sand classes on Vis-NIR predictions of clay and soil organic carbon. *Geoderma* 158:15–22. doi:10.1016/j.geoderma.2010.04.008
- Stuart, B. 2004. *Infrared spectroscopy: Fundamentals and application.* John Wiley & Sons, Chichester, UK.
- Tian, Y., J. Zhang, X. Yao, W. Cao, and Y. Zhu. 2013. Laboratory assessment of three quantitative methods for estimating the organic matter content of soils in China based on visible/near-infrared reflectance spectra. *Geoderma* 202–203:161–170. doi:10.1016/j.geoderma.2013.03.018
- Tomasella, J., and M.G. Hodnett. 1998. Estimating soil water retention characteristics from limited data in Brazilian Amazonia. *Soil Sci.* 163:190–202.
- Tomasella, J., M.G. Hodnett, and L. Rossato. 2000. Pedotransfer functions for the estimation of soil water retention in Brazilian soils. *Soil Sci. Soc. Am. J.* 64:327–338.
- Tranter, G., B. Minasny, A.B. McBratney, R.A. Viscarra Rossel, and B.W. Murphy. 2008. Comparing spectral soil inference systems and mid-infrared spectroscopic predictions of soil moisture retention. *Soil Sci. Soc. Am. J.* 72:1394–1400. doi:10.2136/sssaj2007.0188
- van den Berg, M., E. Klant, L.P. van Reeuwijk, and G. Sombroek. 1997. Pedotransfer functions for the estimation of moisture retention characteristics of Ferralolsols and related soils. *Geoderma* 78:161–180. doi:10.1016/S0016-7061(97)00045-1
- van Genuchten, M.Th. 1980. A close-form equation for predicting the hydraulic conductivity of unsaturated soils. *Soil Sci. Soc. Am. J.* 44:892–898. doi:10.2136/sssaj1980.03615995004400050002x
- Vereecken, H., M. Weynants, M. Javaux, Y. Pachepsky, M.G. Schaap, and M.Th. van Genuchten. 2010. Using pedotransfer functions to estimate the van Genuchten–Mualem soil hydraulic properties: A Review. *Vadose Zone J.* 9:795–820. doi:10.2136/vzj2010.0045
- Vereecken, H., J. Diels, J. Vanorshoven, J. Feyen, and J. Bouma. 1992. Functional evaluation of pedotransfer functions for the estimation of soil hydraulic properties. *Soil Sci. Soc. Am. J.* 56:1371–1378. doi:10.2136/sssaj1992.03615995005600050007x
- Vereecken, H., J. Maes, and J. Feyen. 1990. Estimating unsaturated hydraulic conductivity from easily measured soil properties. *Soil Sci.* 149:1–12. doi:10.1097/00010694-199001000-00001
- Vereecken, H., J. Maes, J. Feyen, and P. Darius. 1989. Estimating the soil moisture retention characteristic from texture, bulk density, and carbon content. *Soil Sci.* 148:389–403. doi:10.1097/00010694-198912000-00001
- Viscarra Rossel, R.A., and T. Behrens. 2010. Using data mining to model and interpret soil diffuse reflectance spectra. *Geoderma* 158:46–54. doi:10.1016/j.geoderma.2009.12.025
- Viscarra Rossel, R.A.V. 2008. ParLeS: Software for chemometric analysis of spectroscopic data. *Chemom. Intell. Lab. Syst.* 90:72–83. doi:10.1016/j.chemolab.2007.06.006
- Viscarra Rossel, R.A., R.N. McGlynn, and A.B. McBratney. 2006a. Determining the composition of mineral-organic mixes using UV-Vis-NIR diffuse reflectance spectroscopy. *Geoderma* 137:70–82. doi:10.1016/j.geoderma.2006.07.004
- Viscarra Rossel, R.A., B. Minasny, P. Roudier, and A.B. McBratney. 2006b. Colour space models for soil science. *Geoderma* 133:320–337. doi:10.1016/j.geoderma.2005.07.017
- Viscarra Rossel, R.A., D.J.J. Walvoort, A.B. McBratney, L.J. Janik, and J.O. Skjemstad. 2006c. Visible, near infrared, mid infrared or combined diffuse reflectance spectroscopy for simultaneous assessment of various soil properties. *Geoderma* 131:59–75. doi:10.1016/j.geoderma.2005.03.007
- Walkley, A.J., and I.A. Black. 1934. An examination of Degtjareff method for determining soil organic matter and a proposed modification of the chromic acid titration method. *Soil Sci.* 37:29–38. doi:10.1097/00010694-193401000-00003
- Weynants, M., H. Vereecken, and M. Javaux. 2009. Revisiting Vereecken pedotransfer functions: Introducing a closed-form hydraulic model. *Vadose Zone J.* 8:86–95. doi:10.2136/vzj2008.0062
- Wetterlind, J., and B. Stenberg. 2010. Near-infrared spectroscopy for within-field soil characterization: Small local calibrations compared with national libraries spiked with local samples. *Eur. J. Soil Sci.* 61:823–843. doi:10.1111/j.1365-2389.2010.01283.x